Materials Physics and Mechanics 42 (2019) 74-102 Received: October 6, 2018

MATHEMATICAL 3D MODELS OF IRREVERSIBLE POLARIZATION PROCESSES OF A FERROELECTRICS AND FERROELASTICS POLYCRYSTAL

A.S. Skaliukh*

Southern Federal University, Rostov-on-Don, Russia

*e-mail: a.s.skaliukh@gmail.com

Abstract. A review of three-dimensional mathematical models describing the irreversible processes of polarization of polycrystalline ferroelectrics is given. Experimental works and most frequently used models for describing hysteresis properties are considered. These include well-known phenomenological and micromechanical models. Some of them allow describing the nonlinear response under the action of electrical and mechanical loads. For each of the models, physical and mathematical features, basic formulas and calculating algorithms are presented. The main advantages and disadvantages of each of the presented models are noted. Large and small loops of dielectric and deformation hysteresis are shown. A conclusion is drawn about the unresolved problems in the field of modeling of polycrystalline ferroelectrics – ferroelastics. The list of works on the review topic is given.
Keywords: mathematical models, ferroelectrics, ferroelastics, hysteresis loops, phenomenological models, micromechanical models

1. Introduction

Since the discovery of the phenomenon of ferroelectricity by Valašek in 1921, almost a century has passed, but the practical significance of this discovery is so great that it is not possible to talk about the completeness of research in this field at the moment. Many ferroelectric materials have been discovered, their structures have been studied, ferroelectric ceramic technologies have been developed, ferroelectrics-relaxors have been discovered, the technologies for creating porous ceramics and composite elements with piezoelectric and magnetic properties have been developed, but the questions of mathematical modeling of non-linear response to electric fields and mechanical stresses remain relevant, and are far from their completion. Technologies of microminiaturization of working elements and thin-film structures put forward new requirements in the field of mathematical modeling of volumetric properties of materials. Indeed, small forces, as well as a small potential difference in such elements, can lead to large mechanical stresses and electric fields that can change the structure of the material due to partial or complete depolarization of the element. And if in the simplest cases it was sufficient to use one-dimensional models that explain the nonlinear hysteresis response of uniaxial (longitudinal) effects, now this is clearly not enough. Models are needed that describe both the longitudinal and transverse response under all possible influences.

The main focus of this review is on polycrystalline ferroelectric materials or ceramics, which are active materials and which, by virtue of their internal structure, have the ability to convert mechanical energy into electrical energy, and *vice versa*. By affecting the sample with

http://dx.doi.org/10.18720/MPM.4212019_8

an electric field or mechanical stress, we observe a response both in the form of electric displacement and in the form of deformation [1].

At small external influences, deformations caused by them and electric displacements are small. Such processes are called reversible. Their modeling is reduced to the construction of constitutive relations in the form of linear algebraic relations connecting external and internal parameters like Hooke's generalized law. In other words, the mathematical model is described by linear algebraic operators, in which the elements of tensors of elastic, piezoelectric and dielectric constants are found experimentally. The calculation of the physical characteristics of the transducers, in which the piezoceramic elements are polarized before saturation, is performed within the framework of these linear models. They are sufficiently studied and include the equations of motion, the equations of electrostatics, geometric relationships and constitutive relationships; to which the initial and boundary conditions are added. In the simplest cases, the equations can be solved analytically, for more complex problems it is convenient to use numerical methods, for example, the finite element method.

The situation changes dramatically as soon as the external loads reach thresholds, and their intensity continues to increase. In this case, irreversible processes start with nonlinear response. And besides with increasing loads, we have someone nonlinear equation, while for decreasing ones we have other. The constitutive relations become not only non-linear but non-single valued. In mathematical terms, they are described by operator relations of hysteresis type. In addition to intense external loads, other parameters, in particular temperature, also affect the irreversibility of the process. For cooling or heat processes, when a temperature changes near a threshold value, called the Curie temperature, a solid phase transition occurs from a low symmetry phase to a high symmetry phase or *vice versa*. However, in this review we present models of irreversible processes of polarization and depolarization by an electric field and mechanical stresses under isothermal processes. Irreversible processes associated with relaxation properties, with the influence of temperature, with the influence of the size of the ferroelectric granules, the dynamics of processes and other features will not be considered here. The main circle of questions will be connected with the analysis of existing mathematical models describing the response of the material to external influences of high intensity for the isothermal process. In other words, the principles of constructing the constitutive relations for irreversible processes of deformation and polarization will be considered, their analysis carried out, and some conclusions formulated.

It is interesting to note that many irreversible processes have a similar response: the relationships between external and internal parameters are mathematically described by similar relationships. In plastic media, the stresses cause elastic and residual strains; in ferromagnetism, the magnetic field leads to induced and remnant magnetization; in ferroelectrics, the electric field generates induced and residual polarization, etc. For cyclic processes, the response is described by hysteresis relationships, as shown in Fig. 1.

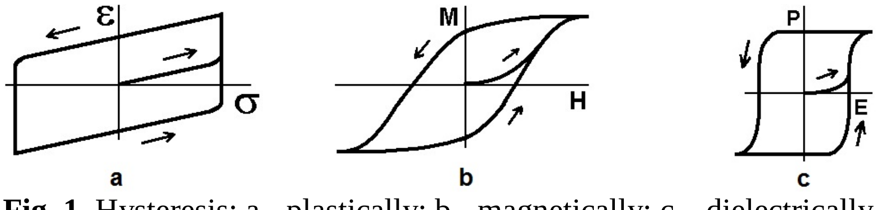

Fig. 1. Hysteresis: a - plastically; b - magnetically; c – dielectrically

Therefore, it happens that the mathematical models developed for someone processes are often used to describe another processes. The closer the observed phenomena in the physical plane, the more accurately the mathematical apparatus works.

Modeling of processes of polarization and depolarization, i.e. the construction of hysteresis-type operators plays an important role in the use of numerical methods for calculating the physical characteristics of the working elements of devices [2]. In particular, in the finite element method, such operators are the constitutive relations closing the system of equations obtained from the laws of continuum mechanics. An important role in modeling is played by experimental data.

2. The main experimental data characterizing the response of the material

The criterion for the correctness and adequacy of the work of any model is a good coincidence of the predicted phenomena with experimental data. A qualitative experiment is a very complex study, so most of them reflect only certain properties with simple effects. The most significant experiments in static tests are those that reflect the complex response of a material due to the action of an electric field and mechanical stresses. Basically, these are the works where the properties of ferroelectric ceramics of the perovskite type are investigated: for example, $BaTiO_3$, or a ceramics containing lead: PZT, PLZT 8/65/35. Interesting results on the response of PLZT 8/65/35 in the complex effect of electric and mechanical fields [3] are shown in Fig. 2.

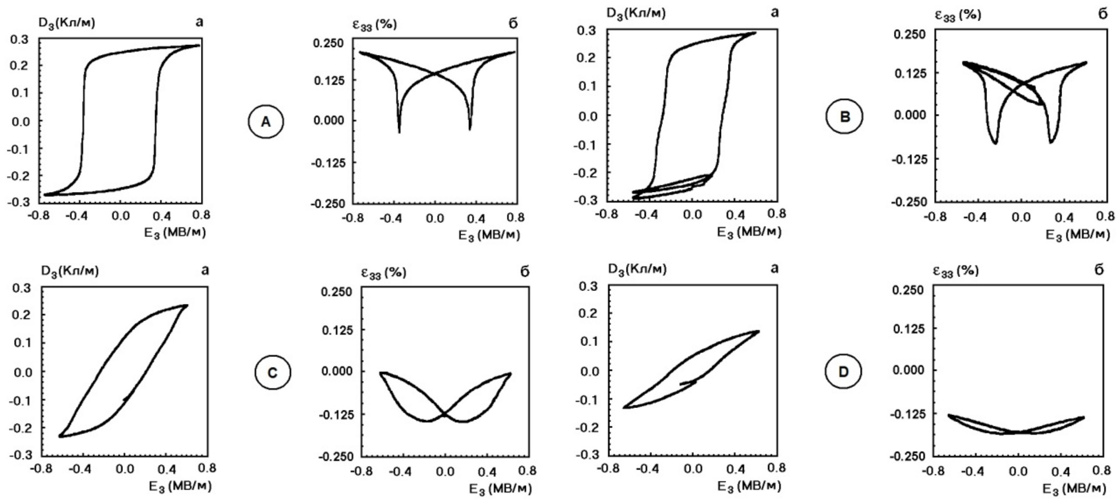

Fig. 2. Full loops of dielectric and deformation type "butterfly" hysteresis for different values of compressive stresses: A - $\sigma = 0\ MPa$; B - $\sigma = -6\ MPa$; C - $\sigma = -30\ MPa$; D - $\sigma = -60\ MPa$

Large loops of dielectric and deformation hysteresis in uniaxial tests and fixed compressive stresses for both lead and lead-free ceramics give similar results [4 – 8] and are shown in Figs. 3, 4.

Conclusion: the loops of the dielectric and deformation hysteresis essentially depend on the intensity of the operating fields. Uniaxial mechanical compressive stresses along the electric field axis affect the ability of domains to rotate. The more intense the mechanical compressive stresses along the field, the less domains the electric field can turn along the line of its action.

As a rule, the mentioned above types of ceramic are the full ferroelectrics-ferroelastics. This means that the strain response to mechanical stresses is also non-linear. The distinctive ferroelastic properties of such materials [6, 8] can be seen in Figs. 5, 6.

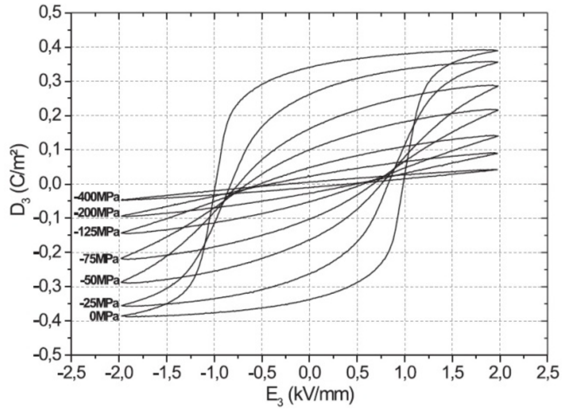

Fig. 3. The effect of compressive stresses on the loop of dielectric hysteresis

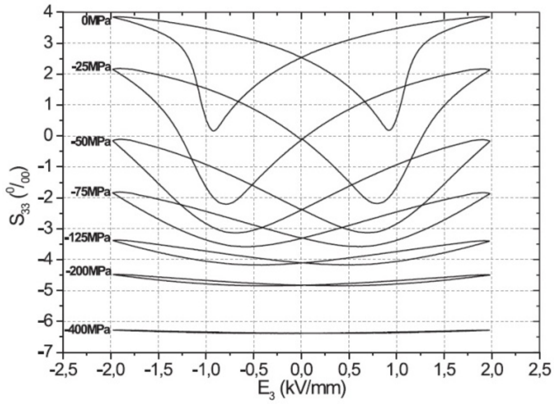

Fig. 4. The effect of compressive mechanical stresses on the strain hysteresis of the butterfly type

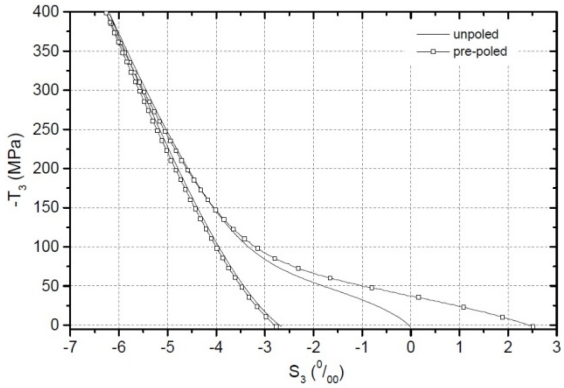

Fig. 5. Small loop $\sigma_{33} \leftrightarrow \varepsilon_{33}$.

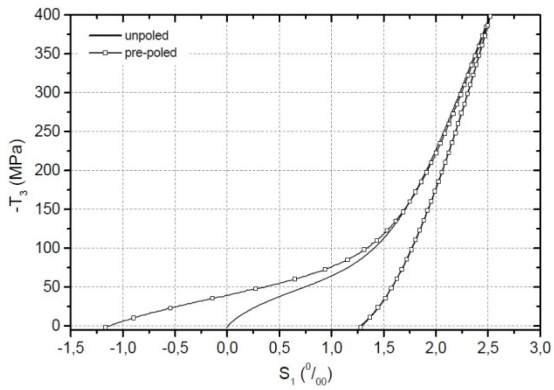

Fig. 6. Small loop $\sigma_{33} \leftrightarrow \varepsilon_{11}$.

Conclusion: for purely mechanical effects, the solid-solid phase transition takes place, the material from isotropic becomes anisotropic, the elastic moduli of the material (tangents to the curves) are changed, and residual deformations appeared that satisfy the condition of incompressibility of material. The last statement can be easily verified if we compare the values of longitudinal and transverse strains.

Dynamic tests, as a rule, are carried out for harmonic impacts. For example, the cyclic effects of an electric field and mechanical stresses can take place both in phase and in anti-phase. The dielectric and deformation loops of such tests [9] are shown in Figs. 7, 8.

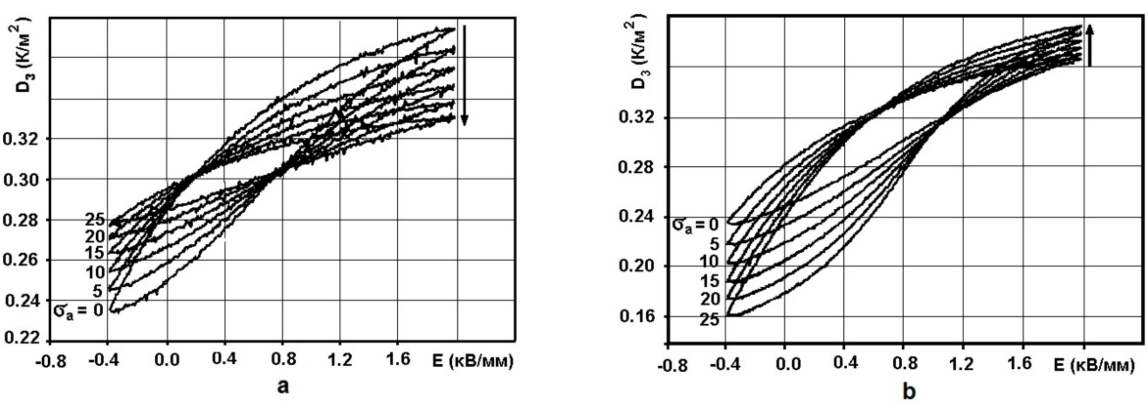

Fig. 7. Dielectric hysteresis for transverse compressive stresses: a – in phase; b – anti-phase

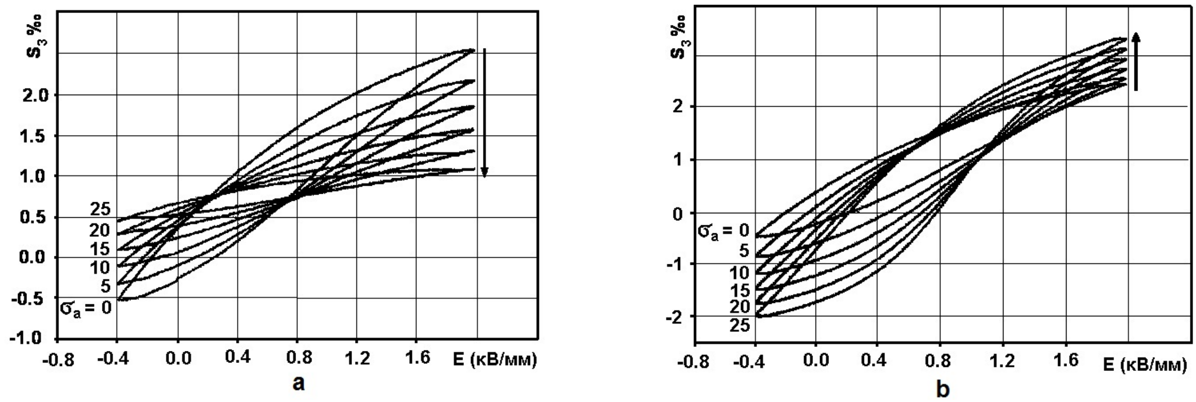

Fig. 8. Strain hysteresis for transverse compressive stresses: a - in phase; b – anti-phase

Conclusion: dielectric and deformation responses at transverse compressive stresses in the phase lead to a decrease in the horizontal slope and a decrease in the area of the loop. Dielectric and deformation responses at transverse compressive stresses in anti-phase lead to an increase in the horizontal slope and increase in the area of the loop.

Along with large loops, small loops of dielectric and deformation hysteresis are often investigated [9]. Such loops of the dielectric and strain hysteresis due to the action of the electric field are shown in Figs. 9, 10. Small loops of strain hysteresis due to the action of mechanical stresses are shown in Figs. 11, 12. Moreover, Fig. 18 reflects the expansion-contraction process, and Fig. 19 – pure compression followed by an increase in intensity.

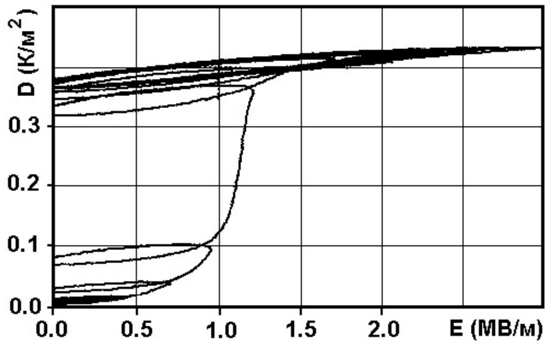

Fig. 9. Dielectric response; small cycles; electric field load

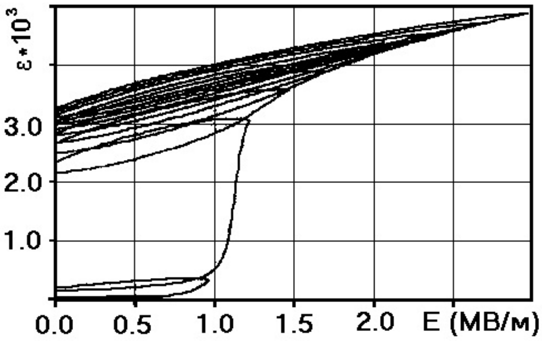

Fig. 10. Strain response; small cycles; electric field load

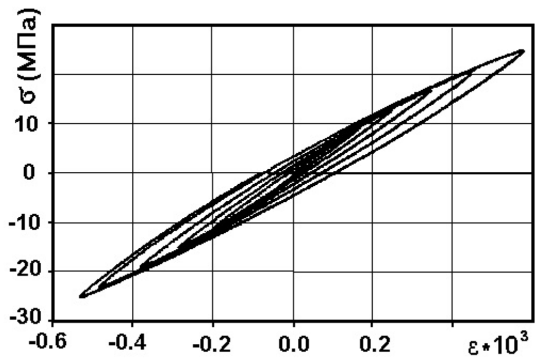

Fig. 11. Dependence of stresses on strains at small cycles with change of sign of strain

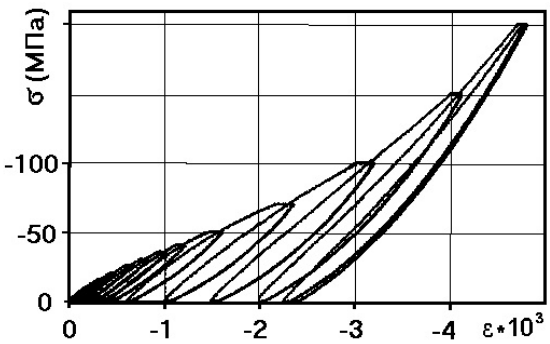

Fig. 12. Dependence of stresses on strains for small cycles without changing the sign of strain

Conclusion: according to small hysteresis loops, one can judge the changing elastic, dielectric and piezoelectric modules of the material.

Summing up, we can say that the main task of mathematical modeling of irreversible processes is the construction of hysteresis operators taking into account the changing anisotropy of material properties.

3. The simplest one-dimensional models

The most common one-dimensional models were numerically investigated in [2]. In the same place, algorithms are described and the results of calculations in the form of plots of dielectric and strain hysteresis loops are presented. Here we briefly mention the basic mathematical principles of models.

The Rayleigh model. This model describes hysteresis by simple parabolic functions. The Rayleigh model [10] was one of the first, in which hysteresis dependences for the magnetization processes of iron are described. In order to apply it to the polarization processes of polycrystalline ferroelectrics, the magnetic field must be replaced by an electric field, and the magnetization by polarization. Mathematically, the branches of the dielectric hysteresis are described by parabolic relationships, as shown in Fig. 13:

$$P = \begin{cases} \alpha E^2, & \textit{initial polarization curve,} \\ \alpha E_{\max} E \pm \dfrac{\alpha}{2}(E_{\max}^2 - E^2), & \textit{descending and ascending branches,} \end{cases}$$

where $\alpha = p_s / E_{\max}^2$, p_s is the spontaneous polarization, $E_{\max}$ is the maximum value of the electric field.

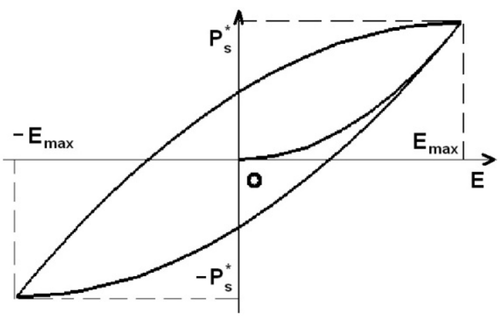

Fig. 13. The Rayleigh model

Obviously, such dependence only approximately describes the hysteresis.

Evolutionary models. This model describes hysteresis phenomena with the help of evolutionary laws leading to hereditary operators. It was developed on the assumption that macroscopic electrical properties are described by a system of electric dipoles, the magnitude and orientation of which can be changed by external loads, and the material in the macroscopic plan is uniform. Dipole dynamics is regulated by an atomic lattice, for which typical times of electronic response are less than 10^{-11} seconds. In [11] it is assumed that the dipole moment μ depends on strain S, absolute temperature θ, electric field E and the number of switching dipoles N in the form of a functional dependence $\mu = \hat{\mu}(S,\theta,E,N)$. And since the process of domain switching has a time scale of the order of 10^{-8} to 10^{-5} seconds, it is considered that the parameter N obeys the evolutionary law. Mechanical stress T and electrical displacement D can be represented by time-independent relationships:

$$T = T^*(S,\theta,E,N); \quad D = D^*(S,\theta,E,N); \quad \dot{N} = h(S,\theta,E,N).$$

Further assumptions are related to the type of introduced functions. In the case when they can be taken as linear, we obtain a hereditary theory of ferroelectricity:

$$T = C(0)(S - S_r) + \int_0^t \frac{d}{dt} C(t-\tau)(S(\tau) - S_r)\, d\tau + \Theta(0)(\theta - \theta_r) +$$

$$\int_0^t \frac{d}{dt} \Theta(t-\tau)(\theta(\tau) - \theta_r)\, d\tau + \eta(0)E + \int_0^t \frac{d}{dt} \eta(t-\tau) E(\tau)\, d\tau;$$

$$D = D_r + L(0)(S - S_r) + \int_0^t \frac{d}{dt} L(t-\tau)(S(\tau) - S_r)\, d\tau + \kappa(0)(\theta - \theta_r) +$$

$$\int_0^t \frac{d}{dt} \kappa(t-\tau)(\theta(\tau) - \theta_r)\, d\tau + \varepsilon(0) + \int_0^t \frac{d}{dt} \varepsilon(t-\tau) E(\tau)\, d\tau.$$

The creep functions entering here are not written out due to the cumbersome nature.

To determine the physical properties of polarized ceramic PZT 65/35, in one-dimensional case [12], the temperature influence is neglected and, under certain conditions, instead of operator relations of the hereditary theory, linear relations are used containing additional terms in elastic, piezoelectric and dielectric modules. A connection was established between the velocities of elastic waves with elastic modules for polarized and unpolarized states, and was added experimentally founded value of the dielectric constant. After that, all parameters are determined. Similar studies can be found in [13–17].

Models of the theory of plasticity. These models qualitatively describe the polarizing effects; they are based on the similarity of the phenomena plasticity and polarization and were constructed using rheological models. The analogy of mechanical and electrical quantities is stated on the base of similar phenomena description: the generalized coordinate – the electric charge; generalized speed – current; coefficient of elastic compliance – capacity; the generalized force – the electromotive force. In the transition to continuous media, forces are replaced by mechanical stresses, displacements by strains, etc. As a result, one can write the following correspondence: $\sigma \leftrightarrow E$, $\varepsilon \leftrightarrow P$, where E is the electric field; P is the polarization or electrical displacement; σ is the mechanical stress; ε is the deformation. The elastic element of Hooke is associated with a condenser, the element of Saint-Venant dry friction is a bipolar zener diode (Fig. 14).

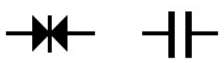

Fig. 14. Condenser and bipolar zener diode

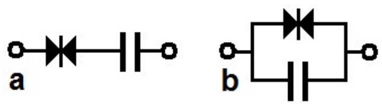

Fig. 15. Connection of elements: a – in series; b – in parallel

In the theory of plasticity, rheological formulas for elastic and plastic deformations are conveniently described by differential inclusions [18]. Therefore, it is natural to extend this apparatus to the theory of polarization. Then for the condenser and zener diode it is convenient to use the expressions:

$$E_e = \frac{1}{c} P_e; \quad E_0 \in rS(\dot{P}_0) \quad (c, r > 0 - const),$$

where the indices "e" and "0" indicate the induced and residual components, respectively, and $S(v)$ is a sets function determined by the rule:

$$S(v) := \begin{cases} \{-1\}, & v < 0; \\ [-1,+1], & v = 0; \\ \{+1\}, & v > 0. \end{cases}$$

The generalization of the model is associated with various compounds of the elements, for example, in series (Fig. 15 a), or in parallel (Fig. 15 b). In the first case, we obtain a differential inclusion that defines the "play" operator. In the second case, we obtain a differential inclusion, which defines the operator "stop" [19,20]. Next, we can determine the Prager polarization models by adding capacitors to the chains considered, as shown in Fig. 16.

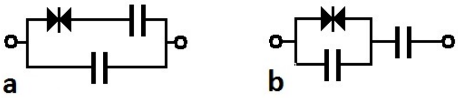

Fig. 16. Polarizing models of Prager: a – capacitor in parallel; b – capacitor in series

Without dwelling on a detailed description of the Prager model, we note only the second case, shown in Fig. 16 b, which is described by the rheological formula [2]:

$$\left(1+\frac{c_1}{c_2}\right)\dot{P}-c_1\dot{E}\in S^{-1}\left(\frac{E-(1/c_2)P}{r}\right)$$

Without dwelling on a detailed description of the Prager model, we note only the second case, shown in Fig. 16 b, which is described by the rheological formula [2]:

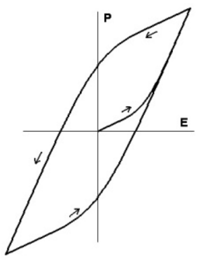

Fig. 17. Generalized model of Prager

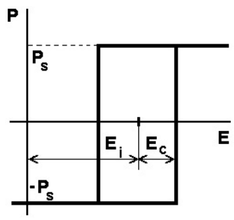

Fig. 18. Hysteron

Varying the parameters of the model, it is possible to substantially change the shape of the hysteresis loop. The main drawback of this model is that with its help it is difficult to describe the saturation state.

The Preisach model. This model uses the rheological model "hysteron" [21,22], which describes the switching of a 180° domain with an increasing and decreasing electric field exceeding the coercive value. In fact, "hysteron" is a generalization of the sets function to the processes of switching a simple 180° domain. The model was proposed in 1935 by F. Preisach [23]. In the simulation of polarization, a set of 180° domains is introduced and the inhomogeneity of the structure is taken into account, according to which there is a large scatter of domains along coercive and internal fields. The switching of each domain is described by a rectangular hysteresis loop with its coercive (E_c) and internal (E_i) fields (Fig. 18).

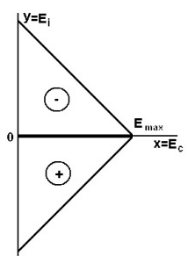

Fig. 19. Diagram Preisach of depolarized ceramics

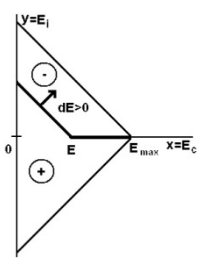

Fig. 20. Diagram Preisach at $dE > 0$

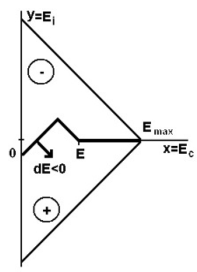

Fig. 21. Diagram Preisach at $dE < 0$

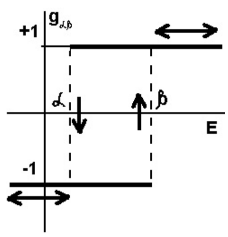

Fig. 22. Relay operator

The presence of a huge number of domains in ceramics allows us to talk about their probability distribution, with a probability density function $\mu(x, y)$ defined on the plane $\{|x| \le \infty, y > \infty\}$:

$$\iint_{x \ge 0} \mu(x, y)dxdy = 1, \quad (x = E_i, y = E_c).$$

For each state in the half-plane there is a boundary separating the domains of two opposite directions. For an unpolarized state, it is the abscissa (Fig. 19). When an electric field of one or another sign is applied these boundary moves due to the involvement of new hysterons in the switching process (Fig. 20). If the electric field changes the direction of growth, then the direction of movement of the boundary also changes (Fig. 21).

The distribution function in the locality of coercive fields has a pronounced peak, which allows us to approximate it using known distributions, with subsequent determination of the parameters entering into it. There are also distribution functions in the form of polynomials in intense and coercive fields [24 – 27].

For a mathematical representation, we introduce the concept of an elementary dipole hysteresis operator (Fig. 22), or the relay operator [20] $\gamma_{\alpha\beta} : C^0[o,T] \times \{-1,+1\} \to \{-1,+1\}$, which is a rate independent one. The parameters α and β for the relay operator and the parameters x and y for the hysteron are related by linear relations: $\alpha = y - x$; $\beta = y + x$, so $\gamma_{y-x,x+y} = \hat{\gamma}_{\alpha\beta}$. The irreversible polarization is determined by the integral

$$P(t) = p_s^* \iiint_{x \ge 0} \mu(x, y)(\hat{\gamma}_{\alpha\beta} E)(t)dxdy,$$

where p_s^* is the maximum polarization value achievable in the process of ceramic polarization by a homogeneous electric field. It is noteworthy that if we choose a uniform distribution function

$$\mu(x, y) = \begin{cases} 1/E_{\max}^2, & if \quad (x, y) \in S_\Delta; \\ 0, & if \quad (x, y) \notin S_\Delta; \end{cases}$$

where S_Δ is the region on the half-plane of the variables x and y, indicated in Fig. 19 by a triangle with hysterons, then by simple calculations of the integrals we easily find hysteresis dependences of the Rayleigh method.

The various shapes of the dielectric hysteresis loops, calculated using the Preisach model, can be found in [2]. The shape and slope of the loops depend strongly on the Gaussian distribution parameters. So for the case

$$\mu(x, y) = \frac{1}{\sqrt{2\pi}\sigma_1} \exp\left[\frac{-(x - a_1)^2}{2\sigma_1^2}\right] \frac{1}{\sqrt{2\pi}\sigma_2} \exp\left(\frac{-y^2}{2\sigma_2^2}\right),$$

where $E_{\max} = 2 \cdot 10^6\ V/m$; $\sigma_1 = \sigma_2 = 2 \cdot 10^2$ (the dimensions of σ_1, σ_2 coincide with the dimensions of x, y), one can investigate the influence of the parameter a_1 (dimensionality x). Assuming successively $a_1 = 0, a_1 = 1 \cdot 10^6, a_1 = 2 \cdot 10^6, a_1 = 5 \cdot 10^6, a_1 = 7 \cdot 10^6$, we obtain the loops shown in Fig. 23.

The Preisach model has become widespread not only in the description of magnetic and ferroelectric hysteresis, but it is intensively used in calculating the damping coefficients of many dynamical systems [28–52], including taking into account the dipole switching dynamics [53–60].

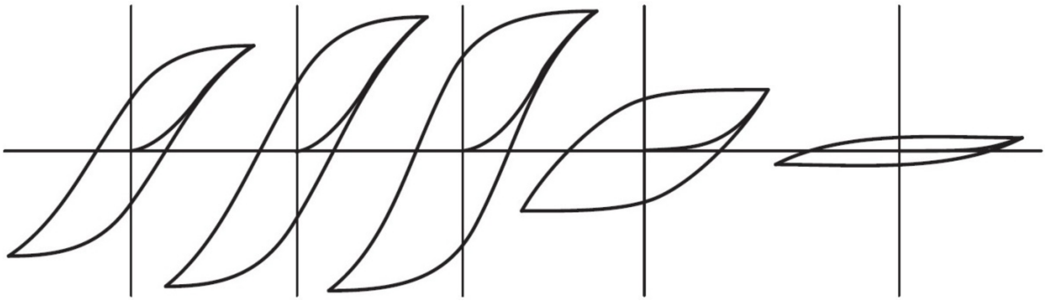

Fig. 23. Preisach model: the effect of increasing the parameter a_1 on the shape of the hysteresis loop

4. Three-dimensional models of polarization

Some three-dimensional models are a simple generalization of one-dimensional models to the 3D-case. These include evolutionary models, plasticity models and the Preysach model. But there are also those that differ fundamentally from those presented earlier. Some of them were described in [2], the other part will be presented below.

Evolutionary model. This model [61] describes hysteresis phenomena with the help of evolutionary laws leading to hereditary operators. In contrast to one-dimensional models, here the dipole moment is a vector quantity and is divided into instantaneous and transient parts: $\boldsymbol{\mu} = \boldsymbol{\mu}_i + \boldsymbol{\mu}_t$. The instant part depends functionally on strain, absolute temperature and electric field $\boldsymbol{\mu}_i = \boldsymbol{\mu}_i(\mathbf{S}, \theta, \mathbf{E})$, and the transition part is related to these parameters and to the vector $\mathbf{N}$ characterizing the number of domains by the evolutionary law. The vector parameter $\mathbf{N}$ also satisfies the evolutionary law:

$$\dot{\boldsymbol{\mu}}_t = \mathbf{f}_{\mu_i}(\mathbf{S}, \theta, \mathbf{E}, \mathbf{N}), \quad \dot{\mathbf{N}} = \mathbf{f}_N(\mathbf{S}, \theta, \mathbf{E}, \mathbf{N}).$$

The constitutive relations for the stress tensor and the electric displacement vector are written in the form of functional relationships:

$$\mathbf{T} = \mathbf{T}^*(\mathbf{S}, \theta, \mathbf{E}, \mathbf{N}); \quad \mathbf{D} = \mathbf{D}^*(\mathbf{S}, \theta, \mathbf{E}, \mathbf{N}).$$

The totality of these equations represents a general evolutionary model. The subsequent simplifications are related to the fact that only the isothermal process is considered, instead of the vector $\mathbf{N}$, only its projection to the axis of the electric field direction is considered, the evolutionary law for the transition part of the dipole moment is divided into two parts separately for strain and the electric field. Then the constitutive relations can be written in the form of a system of linear equations for the components of the corresponding tensors and vectors. In this case elastic, piezoelectric and dielectric constants for polarized ceramics get additional terms, but to avoid cumbersome expressions, they are not given here.

Another approach, based on the analogy between elastic and viscoelastic materials, was proposed in [62]. It is an extension of the Tiersten nonlinear response model [63] to the case of time dependence, for which the constitutive relations are written in the form of viscoelasticity operators.

Models of the theory of plasticity. Because of the similarity of the processes of polarization and plasticity, plasticity models are often used in describing irreversible processes of polarization and deformation, although they are phenomenological and are not related to the microstructure of the material. The polarization vector and the strain tensor consist of an induced (elastic) and a residual (plastic) part $\mathbf{P} = \mathbf{P}_e + \mathbf{P}_0$, $\boldsymbol{\varepsilon} = \boldsymbol{\varepsilon}_e + \boldsymbol{\varepsilon}_0$. The induced components are related to mechanical stresses and electric field by linear relations, generalized to the three-dimensional case:

$$\boldsymbol{\varepsilon}_e = \mathbf{S}(\boldsymbol{\varepsilon}_0, \mathbf{P}_0) : \boldsymbol{\sigma} - \mathbf{d}^T(\boldsymbol{\varepsilon}_0, \mathbf{P}_0) \cdot \mathbf{E}; \qquad \mathbf{P}_e = \mathbf{d}(\boldsymbol{\varepsilon}_0, \mathbf{P}_0) : \boldsymbol{\sigma} + \boldsymbol{\kappa}(\boldsymbol{\varepsilon}_0, \mathbf{P}_0) \cdot \mathbf{E}.$$

The physical characteristics $\mathbf{S},\mathbf{d},\boldsymbol{\kappa}$ depend on the residual parameters. To determine the residual parts, a generalization is carried out from one-dimensional theory to three-dimensional by means of sets functions in the following way. For one hysteron in the one-dimensional case, the boundary $\{E=-E_c,\ E=+E_c\}$ defines an interval within which $E\in(-E_c,\ +E_c)$ there is no switching, and only after its attainment it is possible occurring the switching. In the three-dimensional case, the electric field is a vector quantity $\mathbf{E}=\{E_1,E_2,E_3\}$. The boundary of the segment is turning into the sphere

$$f\equiv E_1^2+E_2^2+E_3^2-E_c^2=0,$$

at achieving which a switch can occur. This description is well suited for single crystals when the field varies along one of the crystallographic axes. However, for polycrystalline ferroelectrics, with increase of the electric field, more and more domains are included in the switching process. To describe this phenomenon, a theory of plasticity with isotropic hardening is used. The surface of polarization changes its dimensions due to the introduction of a function of some parameter, remaining convex. If the increment of the field leads to the movement of the depicting point inside the surface or along a tangent to it, then there is no switching. But if the increment of the field leads to the motion of the depicting point along the normal to the surface, then the switching will occur and, as a consequence, the residual polarization changes. In the one-dimensional theory, a differential inclusion connecting the electric field and the rate of residual polarization was used to determine the rate of residual polarization. In the three-dimensional case, instead, an associated law is formulated, according to which the increment of the residual polarization is directed along the normal to the surface $d\mathbf{P_0}=d\lambda\dfrac{\partial f}{\partial\mathbf{E}}=2d\lambda(E_1\mathbf{i}+E_2\mathbf{j}+E_3\mathbf{k})$. From here $d\lambda=dP_0/2E$, where $dP_0=|d\mathbf{P_0}|$, $E=|\mathbf{E}|$. The increment $\Delta P_0=dP_0$ can be determined from a relationship $P_0=g(E)$ that is easily obtained from experimental data. Really, if $\mathbf{E}=\{0,0,E\}$, and the hysteresis function $P=\varphi(E)$ is gotten, then from $P=P_e+P_0$, and $P_e=\kappa E$, we easily obtain $P_0=g(E)\equiv\varphi(E)-\kappa E$. For quasi-static processes, a sequence of values of the electric field is chosen $\{E_m\}_{m=0}^{M}:E_m=E(t_m)$, whence $dP_{0,m}=g(E_m)-g(E_{m-1})$. The presented scheme was realized in [64] in a slightly different interpretation of the unknown and determining parameters in [65].

In order to take into account the anisotropic hardening associated with changes in the physical characteristics of the material, plasticity models with both isotropic and kinematic hardening are used [66, 67]. The surface of polarization is modified

$$f\equiv(\mathbf{E}-\mathbf{E^B})\cdot(\mathbf{E}-\mathbf{E^B})-E_c^2(P_{0\max})=0,$$

where $\mathbf{E^B}=\alpha\mathbf{P_0}$ is the back field, $E_c(P_0)$ is the hardening field. The parameter α is a material characteristic which will be determined in the future, and the function $E_c(P_0)$ is determined by experimentally. The increment of the residual polarization is determined by the associated law: $d\mathbf{P_0}=d\lambda\dfrac{\partial f}{\partial\mathbf{E}}$, but the coefficient entering here is found by differentiating the equation of the polarization surface, and can be represented as

$$d\lambda=\frac{(\mathbf{E}-\mathbf{E_B})\cdot d\mathbf{E}}{(\mathbf{E}-\mathbf{E_B})\cdot\dfrac{\partial\mathbf{E_B}}{\partial\mathbf{P_0}}\cdot(\mathbf{E}-\mathbf{E_B})+2E_c\dfrac{\partial E_c}{\partial\mathbf{P_0}}\cdot(\mathbf{E}-\mathbf{E_B})}.$$

The first term in the denominator is responsible for the kinematic hardening, and the second term is for isotropic hardening.

In order to take into account the anisotropic hardening associated with changes in the physical characteristics of the material, both mechanical stresses, strains and polarization surface are constructed taking into account not only electrical but also mechanical parameters. The expressions for such a surface include the modified values of the electric field and mechanical stresses, and the surface itself is displaced in space [2, 68]:

$$f \equiv \frac{(\hat{\mathbf{E}}-\alpha\mathbf{P_0})\cdot(\hat{\mathbf{E}}-\alpha\mathbf{P_0})}{E_c^2} - \frac{3}{2}\frac{(\hat{\boldsymbol{\sigma}}-\beta\boldsymbol{\varepsilon}_0):(\hat{\boldsymbol{\sigma}}-\beta\boldsymbol{\varepsilon}_0)}{\sigma_c^2} + \gamma\frac{(\hat{\mathbf{E}}-\alpha\mathbf{P_0})\cdot(\hat{\boldsymbol{\sigma}}-\beta\boldsymbol{\varepsilon}_0)\cdot(\hat{\mathbf{E}}-\alpha\mathbf{P_0})}{E_c^2\sigma_c} +$$
$$\eta\frac{\mathbf{P_0}\cdot(\hat{\boldsymbol{\sigma}}-\beta\boldsymbol{\varepsilon}_0)\cdot(\hat{\mathbf{E}}-\alpha\mathbf{P_0})}{p_{sat}E_c\sigma_c} + \mu\frac{\mathbf{P_0}\cdot(\hat{\boldsymbol{\sigma}}-\beta\boldsymbol{\varepsilon}_0)\cdot\mathbf{P_0}}{p_{sat}^2\sigma_c} - 1 = 0.$$

The constants γ, η, μ entering here must ensure the convexity of the loading function. The parameters α,β are the functions of the intensity of the plastic deformation tensor and the residual polarization vector. Some authors use empirical formulas for their description, choosing parameters to satisfy the experimental data [68 – 73]. The increment of the residual parameters is determined by means of an associated law: $d\mathbf{P_0} = d\lambda\frac{\partial f}{\partial\hat{\mathbf{E}}}$, $d\boldsymbol{\varepsilon}_0 = d\lambda\frac{\partial f}{\partial\hat{\boldsymbol{\sigma}}}$ with the same coefficient. This coefficient is determined after differentiating the equation of the polarization surface, but because of the bulky of the formulas, it is not given here. If we take in the previous expression $\gamma, = 0, \mu = 0$, we obtain an expression for the loading function [70]. An example of loops of dielectric and deformation type "butterfly" hysteresis calculated from the described model from [70] for a certain set of parameters is given in Fig. 24.

The authors of [74] proposed to consider the related problems of polarization and deformation by introducing unconnected two loading functions for the electrical and mechanical parts with the subsequent determination of the two coefficients entering into the associated laws. It was noted in [75 – 80] that, in contrast to plasticity phenomena, where dislocations move for a long time, it is necessary to take into account the saturation state i.e. the state when all domains were switched and the switching process stopped. Therefore, it was suggested to consider four functions, two of which are loading surfaces, and the other two are criteria for the saturation state:

$$f^P(\mathbf{E},\mathbf{P_0}) \equiv \|\mathbf{E} - c^P\mathbf{P_0}\| - E_c,$$
$$h^P(\boldsymbol{\sigma},\mathbf{E},\mathbf{P_0}) = \|\mathbf{P_0}\| - \hat{P}_{sat}(\boldsymbol{\sigma},\mathbf{E},\mathbf{P_0}),$$
$$f^f(\boldsymbol{\sigma},\mathbf{E},\mathbf{P_0},dev\boldsymbol{\varepsilon}_0^{\mathbf{f}}) \equiv \sqrt{3/2}\,\|\boldsymbol{\sigma} - c^f dev\boldsymbol{\varepsilon}_0^{\mathbf{f}}\| - \hat{\sigma}_c(\mathbf{E},\mathbf{P_0}),$$
$$h^f(\mathbf{P_0},dev\boldsymbol{\varepsilon}_0^{\mathbf{f}}) = \sqrt{2/3}\,\|dev\boldsymbol{\varepsilon}_0^{\mathbf{f}}\| - (\varepsilon_{sat} - \sqrt{2/3}\,\|dev\boldsymbol{\varepsilon}_0^{\mathbf{P}}\|).$$

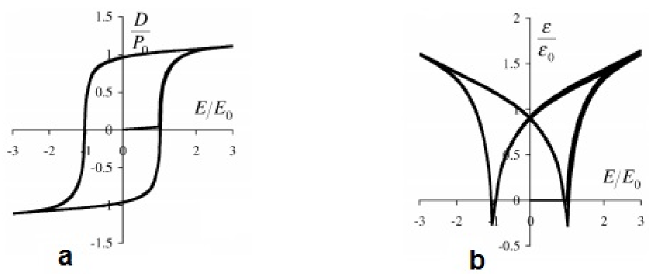

Fig. 24. a – $D \leftrightarrow E$ hysteresis loop; b – $\varepsilon \leftrightarrow E$ butterfly loop

It is assumed that $dev\boldsymbol{\varepsilon}_0$ is the deviator of residual strain tensor, and the residual strain consists of two parts: $\boldsymbol{\varepsilon}_0 = \boldsymbol{\varepsilon}_0^{\mathbf{f}} + \boldsymbol{\varepsilon}_0^{\mathbf{P}}$. The first term corresponds to the strain due to the action of the electric field, and the second term is the strain from the action of mechanical stresses. Associated laws lead to the appearance of four constants, which are found from the equations $df^{P}=0,\ dh^{P}=0,\ df^{f}=0,\ dh^{f}=0$, but because of the cumbersomeness here are not given.

An example of hysteresis curves of the dielectric and deformation type "butterfly" hysteresis according to [77] can be seen in Fig. 25.

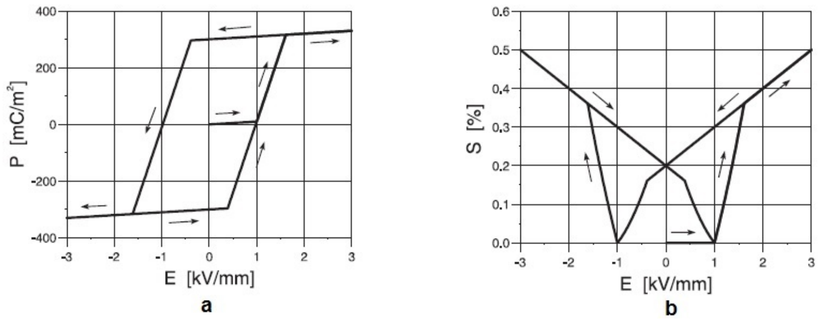

Fig. 25. a – $D \leftrightarrow E$ hysteresis loop; b – $\varepsilon \leftrightarrow E$ butterfly loop

Note that for the generally accepted plasticity models, empirically selected functions $E_c(P_0)$ and others are provided in the calculation of the output of the hysteresis loop to the saturation state. The use of four functions to describe polarization processes lead to the fact that with increasing loads some conditions are replaced by others, and as a consequence, the smoothness of the loops is violated, sharply pronounced angles can appear on the hysteresis curves.

The Preisach model. Generalized Vector Preisach models have developed significantly for magnetization processes, while for polarization processes they are almost not used. The foundations of a simple generalization of the scalar model to the three-dimensional case are laid down in the works of I.D. Mayergoyz [82 – 85], and the main mathematical aspects are presented in [86]. The vector hysteresis model of Preisach is designed as a superposition of scalar models that are continuously distributed along all possible directions, and can be mathematically represented as:

$$\mathbf{f}(t)=\int_0^{2\pi}\int_0^{\pi/2}\mathbf{e}_{\theta\varphi}\left(\iint_{\alpha\ge\beta}\nu(\alpha,\beta,\theta,\varphi)\hat{\gamma}_{\alpha\beta}u_{\theta,\varphi}(t)d\alpha d\beta\right)\sin\theta d\theta d\varphi,$$

where $\mathbf{f}(t)$ is the vector output value; $\mathbf{e}_{\theta\varphi}$ is the unit vector along the direction defined by the spherical coordinates θ,φ; $u_{\theta,\varphi}(t)$ is the projection of the input vector on the direction $\mathbf{e}_{\theta\varphi}$; $\hat{\gamma}_{\alpha\beta}$ is the hysteresis operator described in Section 3. For magnetic (ferroelectric) applications, we have $\mathbf{u}(t)$ as the strength of the magnetic (electric) field; $\mathbf{f}(t)$ is the residual magnetization (polarization) vector. The main idea of the method is that the total magnetization over all planes passing through the vectors of the magnetic field and the chosen direction is counted, and in each switching plane only 180° domains are approximated. It should be noted that for ferroelectric phenomena this model cannot be perceived by a simple analogy between electric and magnetic phenomena, because in ferroelectrics the position of domains is regulated by crystallographic axes. And if the rotation of the magnetization vector is possible for any position of the magnetic field, then for ferroelectrics there is no such possibility.

Models of plastic deformation of crystals (micromechanical models). The description of the model and the results of calculations can be found in [87–98]. Assuming that in the ferroelectric crystal the strain tensor and the polarization vector can be decomposed as a sum of linear (reversible) $\boldsymbol{\varepsilon}_\mathbf{e},\mathbf{P}_\mathbf{e}$ and residual (analogous to plastic) $\boldsymbol{\varepsilon}_\mathbf{0},\mathbf{P}_\mathbf{0}$ components:

$\boldsymbol{\varepsilon} = \boldsymbol{\varepsilon}_{\mathbf{e}} + \boldsymbol{\varepsilon}_{\mathbf{0}}, \mathbf{P} = \mathbf{P}_{\mathbf{e}} + \mathbf{P}_{\mathbf{0}}$, and, taking into account that $\mathbf{D} \equiv \varepsilon_0 \mathbf{E} + \mathbf{P}_{\mathbf{e}} + \mathbf{P}_{\mathbf{0}}$, one can write down the determining equations of the linear piezoelectric response in the form:

$$\boldsymbol{\varepsilon} = \mathbf{S}^{\mathbf{E}} : \boldsymbol{\sigma} + \mathbf{d}^{\mathrm{T}} \cdot \mathbf{E} + \boldsymbol{\varepsilon}_{\mathbf{0}};$$

$$\mathbf{D} = \mathbf{d} : \boldsymbol{\sigma} + \boldsymbol{\kappa}^{\boldsymbol{\sigma}} \cdot \mathbf{E} + \mathbf{P}_{\mathbf{0}}.$$

Here $\boldsymbol{\sigma}, \mathbf{E}, \mathbf{S}^{\mathbf{E}}, \mathbf{d}, \boldsymbol{\kappa}^{\boldsymbol{\sigma}}$ are the stress tensor, the electric field strength vector, the elastic modulus tensor of the crystal, the tensor of the piezoelectric modules of the crystal, and the dielectric constants tensor of the crystal, respectively. In a tetragonal single crystal, six spontaneous polarization orientations are realized (along the positive and negative directions of the three crystallographic axes) therefore in the absence of external loads, the residual components are zero. When external loads are applied ($\boldsymbol{\sigma}, \mathbf{E}$), different domain switches are possible, with the possible implementation of 3D switching systems.

The residual deformation and polarization can be written as the sum of the contributions of individual domains:

$$\boldsymbol{\varepsilon}_{\mathbf{0}} = \sum_{I=1}^{6} c_I \boldsymbol{\varepsilon}_{SI}; \qquad \mathbf{P}_{\mathbf{0}} = \sum_{I=1}^{6} c_I \mathbf{p}_{SI},$$

where c_I is the concentration (volume fraction) of the I domain in a single crystal that satisfies the constraints: $0 \le c_I \le 1, \ \sum_{I=1}^{6} c_I = 1$. Modules $\mathbf{S}^{\mathbf{E}}, \mathbf{d}, \boldsymbol{\kappa}^{\boldsymbol{\sigma}}$ of a single crystal are determined on the base of the modules of individual domains $\mathbf{S}_{\mathbf{I}}^{\mathbf{E}}, \mathbf{d}_{\mathbf{I}}, \boldsymbol{\kappa}_{\mathbf{I}}^{\boldsymbol{\sigma}}$ by relationships that take into account the volume fraction of each domain:

$$\mathbf{S}^{\mathbf{E}} = \sum_{I=1}^{6} c_I \mathbf{S}_{\mathbf{I}}^{\mathbf{E}}, \quad \mathbf{d} = \sum_{I=1}^{6} c_I \mathbf{d}_{\mathbf{I}}, \quad \boldsymbol{\kappa}^{\boldsymbol{\sigma}} = \sum_{I=1}^{6} c_I \boldsymbol{\kappa}_{\mathbf{I}}^{\boldsymbol{\sigma}}.$$

The change in the concentration of the single I - domain of a single crystal is expressed in terms of the rate of switching from a state with an orientation I to a state with orientation J:

$$c_I = \sum_{\alpha=1}^{30} A^{I\alpha} \dot{f}^{\alpha},$$

where $A^{I\alpha} = 1$, if I - domain is the recipient α of the switching system ($\alpha : J \to I$); $A^{I\alpha} = -1$, if I - domain is a donor α switching system ($\alpha : I \to J$); $A^{I\alpha} = 0$ in other cases. The rates of residual strains and polarization can be represented as

$$\dot{\boldsymbol{\varepsilon}}_{\mathbf{0}} = \sum_{I=1}^{6} \dot{c}_I \boldsymbol{\varepsilon}_{SI} = \sum_{\alpha=1}^{30} \dot{f}^{\alpha} \boldsymbol{\mu}_{\alpha} \gamma_{\alpha}; \qquad \dot{\mathbf{P}}_{\mathbf{0}} = \sum_{I=1}^{6} \dot{c}_I \mathbf{p}_{SI} = \sum_{\alpha=1}^{30} \dot{f}^{\alpha} \mathbf{s}_{\alpha} P_{\alpha},$$

where $\boldsymbol{\mu}_{\alpha} = \frac{1}{2}(\mathbf{s}_{\alpha}\mathbf{n}_{\alpha} + \mathbf{n}_{\alpha}\mathbf{s}_{\alpha})$ is the Schmid orientation tensor; $\mathbf{s}_{\alpha}$ is a unit vector in the direction of the polarization change; $\mathbf{n}_{\alpha}$ is a unit vector associated with the axes of the cell; $\gamma_{\alpha}, P_{\alpha}$ are material constants.

To determine the kinematic variables $\dot{f}^{\alpha}$ that play a fundamental role in describing the switching processes, the conditions of thermodynamic constraints are introduced *a priori*. Using the expression for the dissipation power

$$\delta = \boldsymbol{\sigma} : \dot{\boldsymbol{\varepsilon}}_0 + \mathbf{E} \cdot \dot{\mathbf{P}}_0 - \frac{1}{2}(\boldsymbol{\sigma} : \dot{\mathbf{S}}_{\mathbf{I}}^{\mathbf{E}} : \boldsymbol{\sigma} + 2\boldsymbol{\sigma} : \dot{\mathbf{d}}_{\mathbf{I}} \cdot \mathbf{E} + \mathbf{E} \cdot \dot{\mathbf{k}}_{\mathbf{I}}^{\boldsymbol{\sigma}} \cdot \mathbf{E}) = \sum_{\alpha=1}^{30} G^{\alpha} \dot{f}^{\alpha},$$

and taking into account all previous relationships, the driving force is calculated G^{α}:

$$G^{\alpha} = \left[\boldsymbol{\mu}_{\alpha} \gamma_{\alpha} + \frac{1}{2} \sum_{I=1}^{6} A^{I\alpha} (\boldsymbol{\sigma} : \mathbf{S}_{\mathbf{I}}^{\mathbf{E}} + \mathbf{E} \cdot \mathbf{d}_{\mathbf{I}}) \right] : \boldsymbol{\sigma} + \mathbf{E} \cdot \left[\mathbf{s}_{\alpha} P_{\alpha} + \frac{1}{2} \sum_{I=1}^{6} A^{I\alpha} (\mathbf{d}_{\mathbf{I}} : \boldsymbol{\sigma} + \boldsymbol{\kappa}_{\mathbf{I}}^{\boldsymbol{\sigma}} \cdot \mathbf{E}) \right].$$

After this, the evolution equations for finding the kinematic variables $\dot{f}^{\alpha}$ are taken in the form:

$$\dot{f}^{\alpha} = B^{\alpha} \frac{G^{\alpha}}{G_c^{\alpha}} \left| \frac{G^{\alpha}}{G_c^{\alpha}} \right|^{n-1} \left(\frac{c_I^{donor(\alpha)}}{C_0} \right)^m ,$$

but in such a way the condition of non-negativity of dissipation is satisfied $\delta \geq 0$. Here $G_c^{\alpha} > 0, B^{\alpha} > 0, n > 0, m > 0, C_0 > 0$ are material constants that determine the shape of the hysteresis curves; $c_I^{donor(\alpha)}$ is the concentration of the I - domain (the donor α switching system).

To describe the scleronomic behavior, one should choose $n >> 1$, as usual, when analyzing the plasticity of crystals. The introduction of the last factor in the evolution equation allows us to describe the saturation effect and to satisfy the inequalities imposed on the volume fraction of domains. Assuming the uniformity of the mechanical stresses and the electric field at any time $\boldsymbol{\sigma}(t), \mathbf{E}(t)$, it is possible to determine the driving forces G^{α} for any switching system, and then directly the kinematic variables $\dot{f}^{\alpha}$. This model includes 7 parameters $\gamma_{\alpha}, P_{\alpha}, G_c^{\alpha}, B^{\alpha}, n, m, C_0$, which must be chosen from the condition of coincidence of calculated and experimental data.

In [99] generalizations were obtained, in the case when effects of the influence of grain boundaries of a polycrystalline material are taken into account.

For the transition from single crystals to polycrystals, the considered plasticity model of crystals must be supplemented by elements that take into account the mutual influence of the single crystals on each other. To this end, a finite-element (FE) approach was realized in [100] for a representative volume of a polycrystalline material. The set of single crystals for which the previously considered model is valid was described by a system of finite elements. Thus, the interaction of single crystals in the process of loading was accomplished by the interaction of one finite element with another, which is the base of the FE method. Such an approach does not take into account the influence of the grain boundaries, but allows us to operate with a huge number of domains taking account of their mutual influence on each other during switching process. This made it possible to describe in detail both the mutual influence of the crystallites on each other and take into account the micro-stresses under inhomogeneous and cyclic loading, and to find the reduced modules of polarized ceramics.

To evaluate the results of the described model, large dielectric hysteresis loops are given in Fig. 26 and Fig. 27, respectively, from [87] and [100].

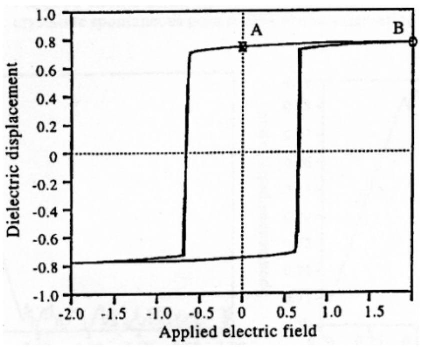

Fig. 26. Dielectric hysteresis loop of single crystal

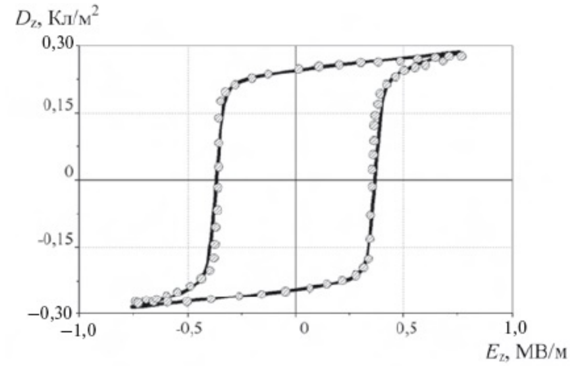

Fig. 27. Dielectric hysteresis loop of polycrystal

Although a somewhat simplified model is presented in [87], it all the same belongs to this class of models, since it operates with the concentration of domains in the crystal.

Comparing these figures, one can draw an important conclusion: in Fig. 26 the loops have almost vertical walls, which are always observed in the polarization of ferroelectric crystals; in Fig. 27 the lateral walls of the loops have a pronounced slope and a smooth transition to the saturation curves, which is inherent in polycrystalline materials.

Model of orientational switching. In this model, a representative volume is considered, which includes a set of domains oriented in space in an arbitrary manner [101]. Not only 180°, but also 90° switching are considered, and the residual polarization vector and the residual strain tensor are determined by simple averaging:

$$\mathbf{P_0} \equiv <\mathbf{p}_S> = \frac{p_S}{N}\sum_k (\mathbf{c})_k; \qquad \boldsymbol{\varepsilon}_\mathbf{0} \equiv <\boldsymbol{\varepsilon}_S> = \frac{\varepsilon_S}{N}\sum_k (\mathbf{c}\otimes\mathbf{c} - \frac{1}{2}\mathbf{a}\otimes\mathbf{a} - \frac{1}{2}\mathbf{b}\otimes\mathbf{b})_k .$$

The orientation of each domain is characterized by crystallographic axes $\mathbf{a}, \mathbf{b}, \mathbf{c}$ (Fig. 28). Let the vector of tenseness of the applied electric field is $\mathbf{E}$. We denote the plane, passing through the origin (the point of reduction) perpendicularity to the axis $\mathbf{c}$ of the domain, as B, and the plane, passing through the vectors $\mathbf{c}$ and $\mathbf{E}$, as A.

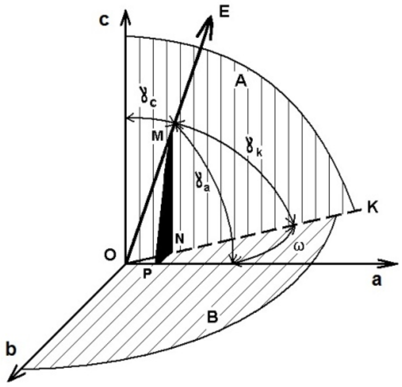

Fig. 28. Determination of angles in the model of orientational switching

The line of intersection of these planes will be a straight line OK. Let us denote γ_k is the smallest of the angles between $\mathbf{E}$ and the line of intersection of the planes. From the four possible directions of the vector $\mathbf{a}$ we choose the one at which it makes the angle closest to the field. We introduce the following angles: γ_c is the angle between the direction of the field and $\mathbf{c}$-axis; γ_a is the angle between the vector $\mathbf{a}$ and the field $\mathbf{E}$; ω is the angle between $\mathbf{a}$-axis and the line of intersection OK. It is obvious that the introduced angles are within

$0 \le \gamma_c \le \pi; \quad 0 \le \omega \le \pi/4; \quad \omega \le \gamma_a \le \pi/2$

Let E_{cc}, E_{ca} are the coercive fields of 180° and 90° switching, respectively. The main conditions are switching (rotations) of domains, which are written in the form of a system of inequalities of 180° rotations:

$$E\cos\gamma_c \ge E_{cc}; \quad \frac{E\cos\gamma_c}{E_{cc}} - \frac{E\cos\gamma_a}{E_{ca}} \ge 0.$$

For 90° rotations, we have $\frac{E\cos\gamma_a}{E_{ca}} - \frac{E\cos\gamma_c}{E_{cc}} \ge 1$, if the domain axis $\mathbf{c}$ is in the upper part of the sphere and $E\cos\gamma_a \ge E_{ca}$; $\frac{E\cos\gamma_a}{E_{ca}} - \frac{E\cos\gamma_c}{E_{cc}} \ge 0$, if the domain axis $\mathbf{c}$ is in the lower part of the sphere.

Dielectric hysteresis loops are constructed for quasi-static processes, i.e. for a sequence of equilibrium states $\{E_i\}$. For this purpose, the process of loading by an electric field $E = E(t)$ is replaced by a sequence of its values $E \in \{E_i\}$: $E_i = E(t_i)$. For each state $E = E_i$, the domain switching conditions are checked, after which the residual polarization and the residual deformation are calculated. Then we have determined the arrangement of the spontaneous polarization vectors for a given vector $\mathbf{E}$, we find the resultant polarization and strain. The dielectric hysteresis loop calculated from this model [2] can be seen in Fig. 29. Taking into account some point as a bringing point, we can assign to each vector of spontaneous polarization a unit vector. The distributions of the spontaneous polarization vectors before and after polarization are shown in Fig. 30.

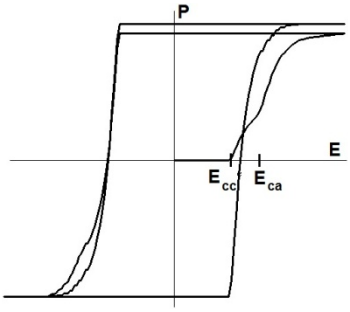

Fig. 29. Hysteresis loop by model of orientational switching

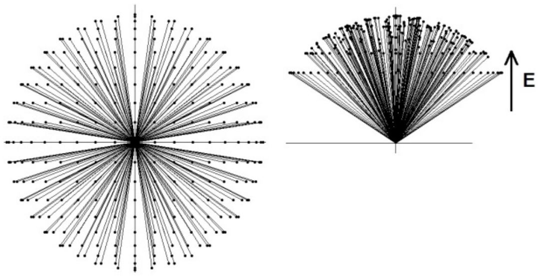

Fig. 30. Distribution of axes before and after polarization

For the calculations, the following values of the parameters included in the model were adopted: $N = 1273248$; $E_{cc} = 2 \cdot 10^6\ V/m$; $E_{ca} = 3 \cdot 10^6\ V/m$; $E_{\max} = 6 \cdot 10^6\ V/m$, where N is the number of spontaneous polarization vectors, E_{cc}, E_{ca} are the coercive fields of 180° and 90° switching, $E_{\max}$ is the maximum value of the electric field. It should be noted that this model allows us to determine the magnitude of the cone angle α in which the directions of the spontaneous polarization vectors are distributed after the removal of the electric field. With the specifying above numerical values of the parameters, we obtained:
$\alpha = 129^0$; $P_{01} = -0.18 \cdot 10^{-4} p_s$; $P_{02} = -0.79 \cdot 10^{-5} p_s$; $P_{03} = 0.81 p_s$.

At physical terms, this model closely adjoins the physics of the phenomenon of polarization of polycrystalline ferroelectrics, but since it does not take into account the mutual influence of domains on each other, it has a "rectangular" loop like at single crystal.

Model of energy switching. This model also considers the representative volume, which includes a set of domains oriented in space in an arbitrary manner [2] and similar to the previous averaging method, the residual polarization vector is determined. The main difference infers in the description of the domain orientation and in the formulation of the domain switching criterion. For ferroelectrics of the perovskite type, the axes of the local system $\mathbf{a}, \mathbf{b}, \mathbf{c}$ are coaxial with the axes of the crystallographic system, as shown in Fig. 31 and with respect to a fixed system $Ox_1x_2x_3$ are determined by means of three angles φ, ψ, ω.

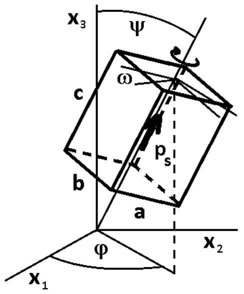

Fig. 31. Assignment the angles of the local coordinate system

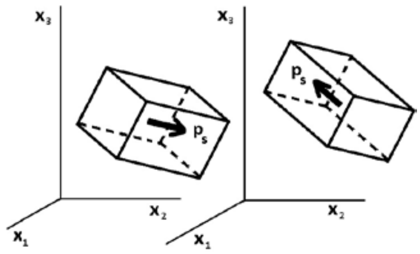

Fig. 32. Possible positions of spontaneous vector. Polarization and deformation of a unit cell

Electric fields and mechanical stresses of high intensity cause a process of domain switching that are compatible with the crystallographic axes of the ferroelectrics, as shown in Fig. 32. With increasing external loads, the energy of each domain varies, but cannot exceed threshold values; switching occurs. If the domain is switched, then only to a position where its energy is minimal, and the switching moment occurs when the difference between the energies of the current state and the state with minimum energy exceeds the threshold value [1, 102, 103]. These conditions form the base of the criterion of energy switching:

$$-\mathbf{p}_S \cdot \mathbf{E} + \mathbf{p}_S^{\min} \cdot \mathbf{E} - \boldsymbol{\varepsilon}_S : \boldsymbol{\sigma} + \boldsymbol{\varepsilon}_S^{\min} : \boldsymbol{\sigma} \geq U_c .$$

Here $\mathbf{E}$ is the electric field vector; $\boldsymbol{\sigma}$ is the tensor of mechanical stresses; U_c is the threshold value of energy.

Dielectric hysteresis loops are also constructed for quasistatic processes. Calculations showed that the form of the loop of dielectric hysteresis exactly coincides with the previous case; therefore, it is not given here. This is to be expected, since only domain switching conditions have changed.

Nevertheless, the energy model of switching has got its application after the appropriate generalization, which consists in taking into account the mutual influence of domains on each other. In [104, 105] it was done by applying the finite element method. The representative volume was divided into a lot of sub regions, taken for domains, and coinciding with finite elements. In each domain, the direction of the crystallographic axes was chosen by the random number sensor, and the direction of spontaneous polarization was set (for ferroelastics, the location of the spontaneous strain tensor was chosen). In a quasistatic process, the energy conditions are checked for each state in each finite element. If they are fulfilled, the domain is switched. After checking all the elements, the transition to the next state is made. The iterative process continues to the last state, which corresponds to the end of the load-unload process. The influence of domains on each other is realized by the mutual influence of finite elements on each other by the mechanical and electric fields. In [104,105] the energy criterion is presented somewhat in a different form, but the mathematical meaning of this has not changed. The results of calculations by the model [105] using the FE method can be seen in Fig. 33, where presented the large dielectric and strain loops of hysteresis.

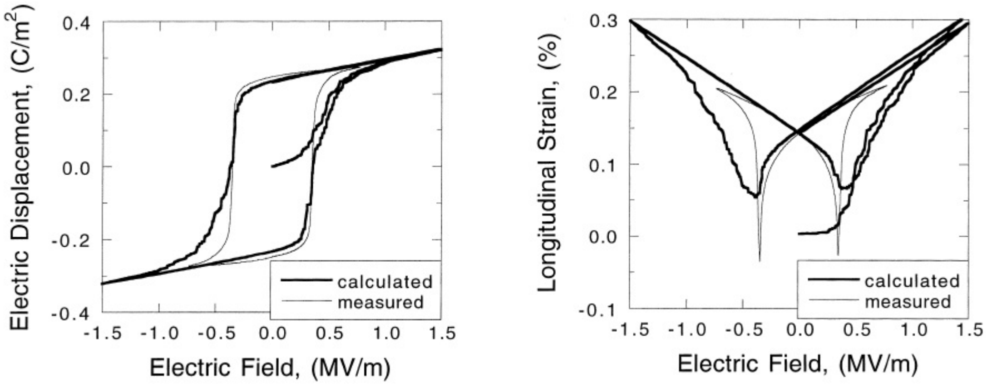

Fig. 33. FE model with an energy switching criterion

The Giles-Atherton model. The model is based on the so-called "limit" (or anhysteretic) curve, derived analytically on the base of Weiss theory and Boltzmann statistics [106 – 113]. If there were no mechanisms for locking (or pinning) the domain walls in the ferroelectric, then after the removal of the electric field the polarization would be zero. This situation is observed in polar liquids, but in polycrystalline ferroelectrics there is a very different mechanism for switching domains. Nevertheless, the basic idea of modeling the polarization process is borrowed from there.

From the mathematical viewpoint, the limiting dependence can be explained and obtained by the methods of mechanics of a multilevel continuum. Let a transition be made from the unpolarized state at zero electric field to the current state with $\mathbf{E} \neq 0$. At the first stage, the micro-level is considered, for which it is supposed that the rotation of domains obeys statistical laws, therefore for a given electric field it is possible to find the distribution of all domains of representative volume. Then averaging is performed (the transition to the macro-level is carried out) and for a representative volume the polarization is obtained. Let assign to each vector of the electric field strength the resulting polarization vector. Since the correspondence is constructed for each transition from the unpolarized state to the current state, we obtain a single-valued dependence, which determines the "limiting" (maximum possible) polarization for a given electric field vector. The implementation of this approach was carried out by Tamm I.E. [106], and briefly it is as follows. Let the unit volume of the dielectric contains N domains with a constant density of the electric moment $\mathbf{p}_s$. Let for each vector of spontaneous polarization one established in compliance the collinear unit vector with beginning in some adducing point in space. The resulting polarization vector is found by determining the area of the unit sphere onto which the ends of the unit vectors exit. In an unpolarized state, all unit vectors are distributed uniformly over the entire surface, so that the resultant polarization is zero.

At the micro-level according to Weiss theory, it is considered that the field of forces acting on the dielectric domain is reduced to the sum of the electric field $\mathbf{E}$ and some "molecular field" proportional to the polarization of the representative volume: $\mathbf{E}^{ef} = \mathbf{E} + \alpha \mathbf{P}_0$, where α is a certain constant that accepts for ferroelectrics large values in comparison with conventional dielectrics.

The fraction of the energy density of a domain that is similar to a dipole depends on the direction of its polarization vector and is expressed by the formula: $U = -\mathbf{p}_s \cdot \mathbf{E}^{ef}$.

According to the theorem of statistical mechanics, the Boltzmann theorem, under the conditions of thermodynamic equilibrium, the law of distribution of domains in the presence of a conservative force field (in this case the electrostatic field) differs from the law of their distribution in the absence of this field by a factor $\exp(-U / k_* T)$, where U is the density of the potential energy of the dipole in the electric field under consideration, T is the absolute temperature, $k_* = 1.38 \cdot 10^{-16}$ erg/deg is a Boltzmann constant. Therefore, the averaging operation yields the maximum possible polarization:

$$\mathbf{P}_\infty = \frac{p_s \int_0^{2\pi} d\varphi \int_0^{\pi} \exp\left(\frac{\mathbf{E}^{ef} \cdot \mathbf{n}_s}{a}\right) \mathbf{n}_s \sin\psi \, d\psi}{\int_0^{2\pi} d\varphi \int_0^{\pi} \exp\left(\frac{\mathbf{E}^{ef} \cdot \mathbf{n}_s}{a}\right) \sin\psi \, d\psi}, \quad \mathbf{p}_s = p_s \mathbf{n}_s, \quad a = \frac{kT}{p_s}.$$

Further actions are carried out at the macro-level for characteristics of a representative volume. As usual, the total polarization consists of two parts: reversible (induced) $\mathbf{P_e}$, and irreversible (residual) $\mathbf{P_0}$:

$$\mathbf{P} = \mathbf{P_e} + \mathbf{P_0}.$$

The reversible part is a state parameter, and it can be defined as some part of the difference from the maximum and residual parts of the polarization:

$$\mathbf{P_e} = c(\mathbf{P}_\infty - \mathbf{P_0}),$$

where c is still an indeterminate factor. The irreversible part of the polarization is the parameter of the process. To determine it, we estimate the energy necessary for breaking the mechanisms pinning the walls of the domain; calculate the work of the electric field in the ideal (limiting) case and count the work of the electric field in the real process of polarization. Further, the energy balance is derived, which can be formulated as follows: the real losses in the process of polarization are formed from losses in the ideal (limiting) case and the energy costs required to break the mechanisms of pinning the walls of the domains. This immediately yields the equation in the differentials for the residual polarization vector:

$$\mathbf{P}_\infty - \mathbf{P_0} = k \frac{d\mathbf{P_0}}{|d\mathbf{E^{ef}}|},$$

where k is a positive constant to be determined. In a quasi-static process, the increment of the residual polarization vector is found numerically for each equilibrium state, after which the total polarization is determined. As a numerical approach the method of Runge-Kutta of the 4th-order gives good results [2]. You can also use the method of successive approximations with an invariable starting point. The latter circumstance is important, because at the same value of the electric field, the increment of the residual polarization vector depends on the direction of the process: as the field increases, we have one monotonic curve, while decreasing, another. When the electric field varies according to the harmonic law, we obtain dielectric hysteresis loops.

The model includes at oneself the 5 parameters: p_s, α, c, a, k, which are selected from the condition of coincidence of calculated and experimental data. In [2], in the one-dimensional case, a lot of numerical experiments were carried out and the effect of the model parameters on the loop shape was investigated. It is shown that the coefficient α is responsible for the amplitude of the loop, the coefficient a for its slope, the coefficient k for the loop area, the coefficient c for the flatness of the loop. Varying the values of the coefficients, one can achieve not only a qualitative but also a quantitative coincidence with the experimental data. For illustration, Fig. 34 shows the effect of the coefficient value on the form of dielectric loops. As the coefficient increases, the slope of the loop increases and its area increases.

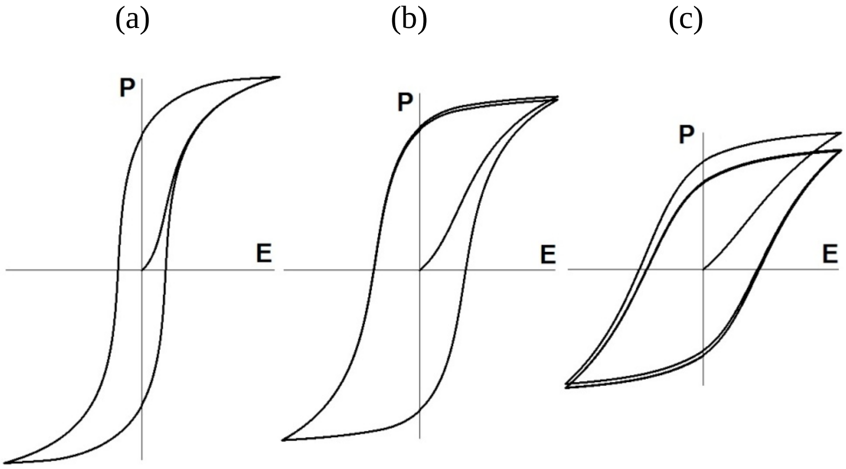

Fig. 34. Giles-Atherton model: (a) $k = 5.1 \cdot 10^5 V/m$; (b) $k = 1.1 \cdot 10^6 V/m$; (c) $k = 2.1 \cdot 10^6 V/m$

This model describes well the large hysteresis loops.

It was shown in [2,114] that the Giles-Atherton model can be generalized to the case of ferroelastics. In [114,115], changes were made to the Giles-Atherton model so to obtain not only large but also small hysteresis loops well coordinated with practice. Without dwelling on the subtleties of the additions, we present only the results of small loops of the dielectric and strain hysteresis in Figs. 35, 36. They agree well with the experimental data shown in Figs. 9, 12, not only qualitatively, but also quantitatively.

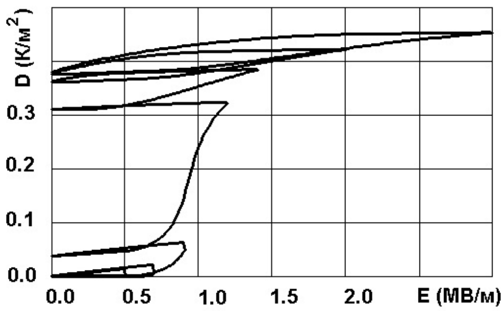

Fig. 35. Small loops $P \leftrightarrow E$

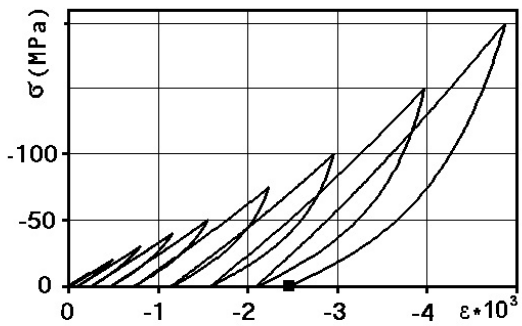

Fig. 36. Small loops $\varepsilon \leftrightarrow \sigma$

In [116,117] one is made a comparison between the Preisach and Giles-Atherton methods, including for the case where models include mechanical stresses.

The considered model of Giles-Atherton by its nature refers to micromechanical models. It uses statistical laws and approaches of a two-level continuum.

5. Discussions

Each of the presented models performs the basic function related to the description of hysteresis dependencies. However, each of them is based on different prerequisites. Therefore, the results of the work of a particular model differ from the corresponding experimental data. Let us evaluate the positive and negative aspects of the models considered.

Phenomenological models: they are models in which functional nonlinearities are formulated for a representative volume. They include the Rayleigh model, evolutionary models and models of the theory of plasticity.

In the Rayleigh model, the nonlinear dependence between the electric field and polarization only approximately describes the dielectric hysteresis, and only for small and medium values of electric field intensity. In evolutionary models, irreversible parameters were introduced in implicit form, for the disclosure of which evolutionary laws were used. Constitutive equations are obtained in the form of integral relations of the theory of viscoelasticity. The creep functions included in the integral relations are constructed for linear functions entering into the evolution equations, the formulation of increasing and falling hysteresis branches being based on inequalities in the functions describing the load and the response of the material. In the models of the theory of plasticity, the main role is played by the surface of polarization (loading), which includes itself a set of input parameters that make it possible to substantially change the shape of the hysteresis loop. Usually, these parameters are chosen so that the results of numerical calculations coincided with the experimental data, as accurately as possible.

Micromechanical models: they are models in which a two-level medium is used to construct the constitutive relationships in a representative volume. Initially the micro-level is considered at the first stage, where threshold loads are taken into account, leading to irreversibility of the proceeding process. Then, in the second stage, by means of averaging, the residual parameters are determined and the constitutive relations for the representative volume are built. The Preisach model, as well as the models plasticity of crystals, energy switching and Giles-Atherton all of them are included in the range of micromechanical models. For each of them, first, at the micro-level, the domain switching conditions are considered, and remaining parameters of the representative volume are found by averaging. In these models, a domain structure is considered in one or another extent.

The Preisach model operates with only 180° domains, and the hysteresis behavior of the functions is based on this. In mathematical terms, the approximation of a real loop is accomplished by elementary rectangular hysteresis loops. The model is intended only for finding the residual polarization, and does not operate with the induced part. In addition, this model does not include mechanical stresses, which significantly reduces its practical application in three-dimensional cases.

The remaining models consider more complete systems of domains. In the models of orientation and energy switching for each domain, a local coordinate system is introduced and the switching conditions are determined, which allows one to move step by step in the direction of irreversibility of the process and obtain an additive picture of the development of the residual parameters.

According to the model of orientational switching, the following conclusions can be drawn. In its essence, it is closer to the physics of the phenomenon of polarization of polycrystalline ferroelectrics, but does not take into account the influence of neighboring domains on each other during the polarization process. Because of this, the loop acquires angular shapes and is not suitable for describing the differential properties of the material. On the other hand, it allows us to find a solution of the angle in which the directions of all the spontaneous polarization vectors are located after reaching the saturation polarization. Another drawback of the model is that it does not include mechanical stresses, which does not allow it to investigate ferroelastic phenomena.

The energy model of switching by physical essence takes into account the physical phenomena of polarization of polycrystalline ferroelectrics, but also does not take into account the effect of neighboring domains on each other during the switching process. The dielectric hysteresis loop has angular shapes. In addition, this model operates only with the residual parameters of polarization and deformation and does not include induced components. However, it has an undeniable advantage, because it includes mechanical stresses, which makes it possible to describe ferroelectric and ferroelastic phenomena. Essential progress in terms of generalization of the model was achieved after applying the finite element method. As soon as each domain was matched with the final element, the effect of the domains on each other was taken into account. This made it possible to obtain good results with satisfactory loops of dielectric and strain hysteresis.

In the Giles-Atherton model, statistical methods are used instead of switching criteria. Analytical expressions were obtained for determining the maximum possible polarization in the form of surface integrals in which the density of the domain distribution is described by functions of exponential type. The integrands were obtained on the base of the energy rotations of the domains as a function of the intensity of the electric field. In this model, the induced component is introduced along with the residual polarization, and the mutual influence of the domains on each other is taken into account twice. Firstly, by means Weiss field, and secondly, for the averaged characteristics in a representative volume, when been take into account the energy costs for breaking the mechanisms pinning the walls of the domain and calculating the work of the electric field in the ideal and real process of polarization. The model contains a set of 5 parameters, by appointing which it is possible to obtain a good coincidence of large hysteresis loops with experimental data. The drawbacks of the model include a very coarse approximation in the description of domain rotations in ferroelectrics, where this process is replaced by the process of rotation of dipoles as in polar liquids in the construction of limiting polarization. This immediately affects when trying to build small hysteresis loops, where the results of calculations lead to large discrepancies. It is noted that the modeling of ferroelastics can be carried out by Giles-Atherton methods if the electric field will be replaced by mechanical stress and a polarization by the strain. The main difference between the Giles-Atherton model and the models considered earlier is that it uses the density function of the domain distribution in the form of analytical integral relations.

6. Conclusions

In summary, three-dimensional theories are divided into phenomenological theories, in which the constitutive relationships are formulated without involving the microstructure of the material, and micromechanical, where such a structure and domain switching processes are taken into account. At first glance it seems that the more accurate the model relies on the physics of the phenomenon, the more accurate the results of its work, however and the phenomenological models give results sufficient to describe irreversible processes. As numerical experiments show, models that include many domains give good results in describing quantitative relationships. How to rule, for it need to select only a few parameters, in contrast to the phenomenological, where it is sometimes necessary to introduce empirical laws. It should be noted that at the moment the universal mathematical model of polarization and deformation of polycrystalline ferroelectric materials has not yet been developed. None of the models considered gives completely identical results with experimental data simultaneously for both large and small hysteresis loops. Some authors prefer one model, and others prefer another, it all depends on the purpose of the study. We can say that there are many unsolved problems that have practical significance. Unresolved problems include the following tasks:

(i) small loops of dielectric and strain hysteresis are not fully investigated;

(ii) in the generally accepted models, all possible effects from the action of each of the components of the stress tensor and the electric field vector are not fully reflected when they are simultaneously acted upon the represented volume;

(iii) there are no studies on how the anisotropy of the material changes with the simultaneous action of an electric field and mechanical stresses, when the direction of the electric field vector does not coincide with any of the principal directions of the stress tensor;

(iv) for quasistatic processes there are no models in which it would be possible to look at the picture of the passage of a domain switching wave along the volume of a ferroelectric;

(v) there are practically no studies related to the analysis of similarities and differences in the existing models of Preisach, Rayleigh, Giles-Atherton, plasticity of materials;
(vi) in fact there is no mathematical analysis of the influence of the model parameters on the final result;
(vii) the methods for selecting the model parameters are poorly represented and there is no formulation of the minimum set of parameters;
(viii) very poorly represented models in which the analytical functions of the density of the distribution of domains would be used, with the subsequent description of hysteresis operators.

Acknowledgements. *This work was supported by the Russian Foundation for Basic Research (Grant 17-08-00860-a).*

References

[1] Hall DA. Review. Nonlinearity in piezoelectric ceramics. *Journal of Materials Science*. 2001;36: 4575-4601.
[2] Belokon AV, Skaliukh AS. *Mathematical Modeling of Irreversible Processes of Polarization*. Moscow: Fizmatlit; 2010. (In Russian)
[3] Lynch CS. The effect of uniaxial stress on the electro-mechanical response of 8/65/35 PLZT. *Acta Metall. mater.* 1996;44(10): 4137-4148.
[4] Dayu Z. *Experimental Investigation of Non-linear Constitutive Behavior of PZT Piezoceramics*. *Dissertation.* Forschungszentrum Karlsruhe GmbH, Karlsruhe; 2003.
[5] Kamlah M, Wang ZA. *Thermodynamically and Microscopically Motivated Constitutive Model for Piezoceramics*. Karlsruhe: FZKA, 2003.
[6] Chen D. *Experimental Investigation of Strain Distributions and Polarization in Lead-based and Lead-free Ferroelectrics*. *Dissertation Doktors der Ingenieurwissenschaften.* Des Karlsruher Instituts für Technologie; 2017.
[7] Zareian Jahromi SA. *Nonlinear Constitutive Modeling of Piezoelectric Materials*. *A thesis submitted to the faculty of graduate studies in partial fulfillment of the requirements for the degree of doctor of philosophy.* Department of mechanical and manufacturing engineering, Calgary; 2013.
[8] Zhou DY, Kamlah M, Munz D. Effects of Bias Electric Fields on the Non-Linear Ferro-Elastic Behavior of Soft Lead Zirconate Titanate Piezoceramics. *Journal of the American Ceramic Society*. 2005;88(4): 867–874.
[9] Zhou DY, Kamlah M, Munz D. Uniaxial compressive stress dependence of the high-field dielectric and piezoelectric performance of soft PZT piezoceramics. *J. Mater. Res.* 2004;19(3): 834-842.
[10] Lord Rayleigh FRS. The behavior of iron and steel under the operation of feeble magnetic forces. *Phil. Mag.* 1887;23: 225-245.
[11] Chen PJ, Peercy PS. One dimensional dynamic electromechanical constitutive relations of ferroelectric materials. *Acta Mechanica*. 1979;31(3-4): 231-241.
[12] Chen PJ, Tucker TJ. Determination of the polar equilibrium properties of the ferroelectric ceramic PZT 65/35. *Acta Mechanica*. 1981;38(3-4): 209-218.
[13] Chen PJ, Montgomery ST. A macroscopic theory for the existence of the hysteresis and butterfly loops in ferroelectricity. *Ferroelectrics*. 1980;23(3): 199-208.
[14] Chen PJ, Tucker TJ. One dimensional polar mechanical and dielectric responses of the ferroelectric ceramic PZT 65/35 due to domain switching. *Int. J. Eng. Sci*. 1981;19(1): 147-158.
[15] Bailey PB, Chen PJ. Transient electromechanical responses of ferroelectric ceramics to impulsive electric fields. *Int. J. Solid and Struct*. 1981;17: 471-478.

[16] Chen PJ, Madsen MM. One dimensional polar responses of the electrooptic ceramic PLZT 7/65/35 due to domain switching. *Acta Mechanica*. 1981;41(3-4): 255-264.
[17] Chen PJ. *Hysteresis Effects in Deformable Ceramics*. In: Maugin GA. (ed.) The mechanical behavior of electromagnetic solid continua (IUTAM). North-Holland, Amsterdam: Elsevier Science Publishers; 1984. p.137-143.
[18] Filatov OP, Khapaev MM. *Averaging of systems of differential inclusions: Textbook*. Moscow: Publishing House of Moscow University; 1998. (In Russian)
[19] Palmov VA. *Oscillations of elastic-plastic bodies*. Moscow: Nauka; 1976. (in Russia)
[20] Visintin A. On hysteresis in elasto-plasticity and in ferromagnetism. *International Journal of Non-Linear Mechanics*. 2002;37(8): 1283–1298.
[21] Visintin A. Quasilinear first-order PDEs with hysteresis. *J. Math. Anal. Appl*. 2005;312(2): 401-419.
[22] Visintin A. Quasilinear Hyperbolic Equations with Hysteresis. *Annales de l'Institut Henri Poincare (C) Non Linear Analysis.* 2002;19(4): 451-476.
[23] Preisach F. Uber die magnetische nachwirkung. *Zeitschrift fur Physik.* 1935;94(5-6): 277–302. (In German)
[24] Robert G, Damjanovic D, Setter N. Preisach distribution function approach to piezoelectric nonlinearity and hysteresis. *J. of Appl. Phys*. 2001;90(5): 2459-2464.
[25] Robert G, Damjanovic D, Setter N. Preisach modelling of ferroelectric pinched loops. *Applied Physics Letters*. 2000;77(26): 4413-4415.
[26] Robert G, Damjanovic D, Setter N, Turik AV. Preisach modeling of piezoelectric nonlinearity in ferroelectric ceramics. *J. of Appl. Phys*. 2001;89(9): 5067-5074.
[27] Turik AV. To the theory of polarization and hysteresis of ferroelectrics. *Solid State Physics*. 1963;5(4): 1213-1215.
[28] Szabo Z, Tugyi I, Kadar G, Fuzi J. Identification procedures for scalar Preisach model. *Physica B*. 2004;343(1-4): 142-147.
[29] Azzerboni B, Cardelli E, Finocchio G. A comparative study of Preisach scalar hysteresis models. *Physica B*. 2004;343(1-4): 164-170.
[30] Dumitru I, Sandu DD. The affect of relaxation phenomena upon the ferromagnetic resonance of fine particle systems. *Journal of Magnetism and Magnetic Materials*. 2003;265(1): 54-59.
[31] Ragusa C. An analytical method for the identification of the Preisach distribution function. *Journal of Magnetism and Magnetic Materials*. 2003;254-255: 259-261.
[32] Borcia ID, Spinu L, Stancu Al. Simulation of magnetization curves with Preisach–Neel models. *Journal of Magnetism and Magnetic Materials*. 2002;242-245: 1034-1037.
[33] Stancu A, Stoleriu L, Cerchez M, Postolache P, Cimpoiesu D, Spinu L. Standard problems for phenomenological Preisach-type models. *Physica B*. 2001;306(1-4): 91-95.
[34] Fuzi J. Strong coupling in electromechanical computation. *Journal of Magnetism and Magnetic Materials*. 2000;215-216: 746-748.
[35] Bottauscio O, Chiampi M, Chiarabaglio D, Repetto M. Preisach-type hysteresis models in magnetic field computation. *Physica B*. 2000;275(1-3): 34-39.
[36] Kadar G. On the product Preisach model of hysteresis. *Physica B*. 2000;275(1-3): 40-44.
[37] Cardelli E, Torre ED, Ban G. Experimental determination of Preisach distribution functions in magnetic cores. *Physica B*. 2000;275(1-3): 262-269.
[38] Vandenbossche L, Dupre L, Melkebeek J. Preisach-based magnetic evaluation of fatigue damage progression. *Journal of Magnetism and Magnetic Materials*. 2005;290-291: 486-489.
[39] Stancu A, Stoleriu L, Postolache P, Tanasa R. New Preisach model for structured particulate ferromagnetic media. *Journal of Magnetism and Magnetic Materials*. 2005;290-291: 490-493.

[40] Carpentieri M, Finocchio G, La Foresta F, Azzerboni B. State-independent hypothesis to model the behavior of magnetic materials. *Journal of Magnetism and Magnetic Materials*. 2004;280(2-3): 158-163.
[41] Korman CE, Della Torre E. Definition of the magnetic ground state using Preisach-based aftereffect models. *Physica B*. 2000;275(1-3): 28-33.
[42] Hu H, Mrad RB. On the classical Preisach model for hysteresis in piezoceramic actuators. *Mechatronics*. 2003;13(2): 85-94.
[43] Liu J, Zhang S, Chen F, Yang C, Zhou X. Measurements and simulation of hysteresis loops of donor-doped strontium bismuth tantalate ceramics. *Physics Letters A.* 2004;321(3): 199-204.
[44] Meyer V, Sallese J-M, Fazan P, Bard D, Pecheux F. Modeling the polarization in ferroelectric materials: a novel analytical approach. *Solid-State Electronics*. 2003;47(9): 1479-1486.
[45] Hu H, Mrad RB. On the classical Preisach model for hysteresis in piezoceramic actuators. *Mechatronics*. 2003;13(2): 85-94.
[46] Yu Y, Naganathan N, Dukkipati R. Preisach modelling of hysteresis for piezoceramic actuator system. *Mechanism and machin theory*. 2002;37(1): 49-59.
[47] Haddad WM, Chellaboina V, Oh J. Linear controller analysis and design for systems with input hysteresis nonlinearities. *Journal of the Franklin Institute*. 2003;340(5): 371-390.
[48] Chuntao L, Yonghong T. A neural networks model for hysteresis nonlinearity. *Sensors and Actuators A*. 2004;112(1): 49-54.
[49] Sjostrom M. Differentiation and power loss computation of classical Preisach model. *Physica B*. 2004;343(1): 96-100.
[50] Pasco Y, Berry A. Consideration of piezoceramic actuator nonlinearity in the active isolation of deterministic vibration. *Journal of Sound and Vibration*. 2006;289(3): 481-508.
[51] Gentili G, Giorgi C. A new model for rate-independent hysteresis in permanent magnets. *International Journal of Engineering Science*. 2001;39(9): 1057-1090.
[52] Kadar G, Szabo G. Hysteresis modeling. *Journal of Magnetism and Magnetic Materials*. 2000;215-216: 592-596.
[53] Fuzi J. Experimental verification of a dynamic hysteresis model. *Physica B*. 2004;343(1-4): 80-84.
[54] Zirka SE, Moroz YI, Marketos P, Moses AJ. Properties of dynamic Preisach models. *Physica B*. 2004;343(1-4): 85-89.
[55] Morentin FJ, Alejos O, Francisco C, Munoz JM, Hernandez-Gomez P, Torres C. Simple standard problem for the Preisach moving model. *Physica B*. 2004;343(1-4): 107-111.
[56] Cheng KWE, Lee WS, Tang CY, Chan LC. Dynamic modelling of magnetic materials for high frequency applications. *Journal of Materials Processing Technology*. 2003;139(1-3): 578-584.
[57] Fuzi J, Kadar G. Frequency dependence in the product Preisach model. *Journal of Magnetism and Magnetic Materials*. 2003;254-255: 278-280.
[58] Cardelli E, Bertoncini F, Di Fraia S, Tellini B. Implementation of the modified Preisach scalar model in the finite difference - time - domain numerical modeling. *Physica B*. 2001;306(1-4): 126-131.
[59] Belbas SA, Mayergoyz ID. Optimal control of dynamical systems with Preisach hysteresis. *International Journal of Non-Linear Mechanics*. 2002;37(8): 1351-1361.
[60] Cross R, Krasnoselskii AM, Pokrovskii AV. A time-dependent Preisach model. *Physica B*. 2001;306(1-4): 206-210.
[61] Chen PJ. Three dimensional dynamic electromechanical constitutive relations of ferroelectric materials *Int. J. Solids and Structures*. 1980;16(12): 1059-1067.

[62] Sohrabi A, Muliana A. Nonlinear Hysteretic Response of Piezoelectric Ceramics. In: Lallart M. (ed.) *Ferroelectrics - Characterization and Modeling*. InTechOpen; 2011. p.537-560. Available from: https://www.intechopen.com/books/ferroelectrics-characterization-and-modeling/nonlinear-hysteretic-response-of-piezoelectric-ceramics [Accessed 26th March 2019].

[63] Tiersten HF. Electroelastic Equations for Electroded Thin Plates Subject to Large Driving Voltages. *J. Applied Physics*. 1993;74: 3389-3393.

[64] Sze KY, Pan Y-S. Nonlinear fracture analysis of piezoelectric ceramics by finite element method. *Engineering Fracture Mechanics.* 2001;68(11): 1335-1351.

[65] Kamlah M, Tsakmakis C. Phenomenological modeling of the non-linear electro-mechanical coupling in ferroelectrics. *International Journal of Solids and Structures*. 1999;36(5): 669-695.

[66] Haug A, Knoblauch V, McMeeking RM. Combined isotropic and kinematic hardening in phenomenological switching models for ferroelectric ceramics. *International Journal of Engineering Science*. 2003;41(8): 887-901.

[67] Muller R, Schroder J, Lupascu DC. Thermodynamic consistent modelling of defects and microstructures in ferroelectrics. *GAMM-Mitt*. 2008;31(2): 133-150.

[68] McMeeking RM, Landis CM. A phenomenological multi-axial constitutive law for switching in polycrystalline ferroelectric ceramics. *International Journal of Engineering Science*. 2002;40(14): 1553-1577.

[69] Huber JE, Fleck NA. Multi-axial electrical switching of a ferroelectric: theory versus experiment. *Journal of the Mechanics and Physics of Solids*. 2001;49(4): 785-811.

[70] Landis CM. Fully coupled, multi-axial, symmetric constitutive laws for polycrystalline ferroelectric ceramics. *Journal of the Mechanics and Physics of Solids*. 2002;50(1): 127-152.

[71] Huber JE, Fleck NA, Landis CM, McMeeking RM. A constitutive model for ferroelectrics. *Journal of the Mechanics and Physics of Solids*. 1999;47(8): 1663-1697.

[72] Huber J, Fleck NA. Multiaxial models and experiments with ferroelectrics. In: Lynch CS. (ed.) *Proceedings Volume 3992, Smart Structures and Materials 2000: Active Materials: Behavior and Mechanics*. SPIE; 2000. Available from; doi:10.1117/12.38821.

[73] Landis CM. Symmetric constitutive laws for polycrystalline ferroelectric ceramics. In: Lynch CS. (ed.) *Proceedings Volume 4333, Smart Structures and Materials 2001: Active Materials: Behavior and Mechanics.* SPIE; 2001. Available from: doi: 10.1117/12.432765.

[74] Elhadrouz M, Zineb TB, Patoor E. Constitutive Law for Ferroelastic and Ferroelectric Piezoceramics. *Journal of Intelligent Material Systems and Structures*. 2005;16(3): 221-236.

[75] Kamlah M, Tsakmakis C. Phenomenological modeling of the non-linear electromechanical coupling in ferroelectrics. *International Journal of Solids and Structures* 1999;36(5): 669-695.

[76] Kamlah M, Bohle U, Munz D. On a non-linear finite element method for piezoelectric structures made of hysteretic ferroelectric ceramics. *Computational Materials Science*. 2000;19(1-4): 81-86.

[77] Kamlah M, Bohle U. Finite element analysis of piezoceramic components taking into account ferroelectric hysteresis behavior. *International Journal of Solids and Structures*. 2001;38(4): 605-633.

[78] Kamlah M, Bohle U. On a non-linear finite element method for piezoelectric structures made of hysteretic ferroelectric ceramics. In: Lynch CS. (ed.) *Proceedings Volume 3992, Smart Structures and Materials 2000: Active Materials: Behavior and Mechanics.* SPIE; 2000. Available from: doi:10.1117/12.388209.

[79] Kamlah M. Ferroelectric and ferroelastic piezoceramics – modeling of electromechanical hysteresis phenomena. *Continuum Mechanics and Thermodynamics*. 2001;13(4): 219-268.

[80] Kamlah M, Jiang Q. A Constitutive Model for Ferroelectric PZT Ceramics Under Uniaxial Loading. *Smart Materials and Structures*. 1999;8(4): 441-459.
[81] Laskewitz B, Kamlah M. Finite element implementation of nonlinear constitutive models for piezoceramic materials. *Journal of mechanics of materials and structures*. 2010;5(1): 19-45.
[82] Mayergoyz ID, Fiedman G. *IEEE Transactions on magnetic*. 1988;24(6): 2928-2930.
[83] Friedman G, Mayergoyz ID. Computation of magnetic field in media with hysteresis. *IEEE Transactions on magnetic*. 1989;25(5): 3934-3936.
[84] Mayergoyz ID. *Mathematical Models of Hysteresis*. New York: Springer-Verlag; 1991.
[85] Frydrych P, Szewczyk R, Nowicki M, Charubin T. Application of Anisotropic Vector Preisach Model for Bulk Materials. *Acta physica polonica A*. 2017;131(4): 618-620.
[86] Visintin A. Vector Preisach model and Maxwell's equations. *Physica B*. 2001;306(1-4): 21-25.
[87] Huo Y, Jiang Q. Modeling of domain switching in polycrystalline ferroelectric ceramics. *Smart Mater. Struct*. 1997;6(4): 441-447.
[88] Huo Y, Jiang Q. Modeling of domain switching in ferroelectric ceramics: an example. *Int. J. Solids Structures*. 1998;35(13): 1339-1353.
[89] Huber JE, Fleck NA, Landis CM, McMeeking RM. A constitutive model for ferroelectric polycrystals. *J. Mech. Phys. Solids*. 1999;47(8): 1663–1697.
[90] Huber JE, Fleck NA. Multi-axial electrical switching of a ferroelectric: theory versus experiment. *Journal of Mechanics and Physics of Solids*. 2001;49(4): 785-811.
[91] Kamlah M, Liskowsky AC, McMeeking RM, Balke H. Finite element simulation of a polycrystalline ferroelectric based on a multidomain single crystal switching model. *International Journal of Solids and Structures*. 2005;42(9-10): 2949-2964.
[92] Huber JE, Fleck NA. Ferroelectric switching: a micromechanics model versus measured behavior. *European Journal of Mechanics A/Solids.* 2004;23(2): 203–217.
[93] Jayabal K, Menzel A, Arockiarajan A, Srinivasan SM. Micromechanical modelling of switching phenomena in polycrystalline piezoceramics. Application of a polygonal finite element approach. *Computational Mechanics*. 2011;48(4): 499-514.
[94] Haug A, Onck PR, Van der Giessen E. Development of inter- and intragranular stresses during switching of ferroelectric polycrystals. *International Journal of Solids and Structures*. 2007;44(6): 2066–2078.
[95] Daniel L, Hall DA, Withers PJ. A multiscale model for reversible ferroelectric behavior of polycrystalline ceramics. *Mechanics of Materials*. 2014;71: 85–100.
[96] Pane I, Fleck NA, Chu DP, Huber JE. The influence of mechanical constraint upon the switching of a ferroelectric memory capacitor. *European Journal of Mechanics A/Solids*. 2009;28(2): 195–201.
[97] Enderlein M, Kuna M, Ricoeur A. A micromechanical material model for ferroelectrics and its application to crack problems. In: Schr¨oder J, Lupascu D, Balzani D. (eds.) *Proceedings of the First Seminar on "The Mechanics of Multifunctional Materials"*. University of Duisburg-Essen; 2007. p.21-25.
[98] Kamlah M, Laskewitz B, Zhou D. Ferroelectric ceramics: basic properties and modeling methods. In: Schr¨oder J, Lupascu D, Balzani D. (eds.) *Proceedings of the First Seminar on "The Mechanics of Multifunctional Materials".* University of Duisburg-Essen; 2007. p. 60-63.
[99] Jayabal K, Arockiarajan A, Sivakumar SM. A Micromechanical Model for Polycrystal Ferroelectrics with Grain Boundary Effects. *Computer Modeling in Engineering & Sciences*. 2008;27(2): 111-124.
[100] Osipova NG, Semyonov AS. The simulation of nonlinear behavior for ferroelectric ceramics with tetragonal structure by finite-element homogenizing. *Scientific and technical*

statements of Saint-Petersburg State Polytechnic University. Physics and mathematics sciences. 2011;4(134): 56-64.
[101] Fesenko EG, Danziger AY, Kramarov OP. *Polarization of ceramics*. Rostov on Don: Publishing house of Rostov State University; 1968. (In Russian)
[102] Skaliukh A. About hysteretic operators arising in the modelling of the polarization of ferroelectric materials. In: *Proceedings of the International Conference on Mathematical Sciences, July 17-19, Chennai, India, Sathyabama university*. Elsevier; 2014. p.635-638.
[103] Shindo Y, Narita F, Horiguchi K, Magara Y, Yoshida M. Electric fracture and polarization switching properties of piezoelectric ceramic PZT studied by the modified small punch test. *Acta Materialia*. 2003;51(16): 4773-4782.
[104] Hwang SC, McMeeking RM. A finite element model of ferroelastic polycrystals. *International Journal of Solids and Structures*. 1999;36(10): 1541-1556.
[105] Hwang SC, Waser R. Study of electrical and mechanical contribution to switching in ferroelectric/ferroelastic polycrystals. *Acta Materialia*. 2000;48(12): 3271-3282.
[106] Tamm IE. *Fundamentals of the theory of electricity: Textbook for high schools.* 11th ed. Moscow: FIZMATLIT; 2003. (In Russian)
[107] Jiles DC, Atherton DL. Theory of magnetic hysteresis. *Journal of Magnetism and Magnetic Materials*. 1986;61(1-2): 48-60.
[108] Sadowski N, Batistela NJ, Bastos JPA, Lajoie-Mazenc M. An inverse Jiles - Atherton model to take into account hysteresis in time-stepping finite-element calculations. *IEEE Trans. on Magn*. 2002;38(2): 797-800.
[109] Jiles DC. *Introduction to magnetism and magnetic materials*. New York: Chapman and Hall; 1991.
[110] Smith RC. A nonlinear optimal control method for magnetostrictive actuators. *Journal of Intelligent Material Systems and Structures*. 1998;9(6): 468-486.
[111] Smith RC, Hom CL. A domain wall model for ferroelectric hysteresis. In: *Proceedings Volume 3667, Smart Structures and Materials 1999: Mathematics and Control in Smart Structures*. SPIE; 1999. Available from: doi:10.1117/12.350070.
[112] Smith RC, Hom CL. A domain wall theory for ferroelectric hysteresis. Center for Research in Scientific Computation (CRSC) technical report CRSC-TR99-01. *Journal of Intelligent Material Systems and Structures*. 1999;10(3): 195-213.
[113] Smith RC, Ounaies Z. A Domain Wall Model for Hysteresis in Piezoelectric Materials. *Journal of Intelligent Material Systems and Structures*. 2000;11(1): 62-79.
[114] Skaliukh A, Belokon A. Modeling strain and dielectric hysteretic type dependences in polycrystalline ferroelectrics by methods of two-level continuum. *Journal of Physics: IOP Conference Series*. 2015;602(1): 012025.
[115] Skaliukh AC. Modeling of Polarization of the Polycrystalline Ferroelectrics. In: Parinov IA. (ed.) *Piezoceramic materials and devices.* NOVA Publishers: NY; 2012. p.55-104.
[116] Benabou A, Clenet S, Piriou F. Comparison of Preisach and Jiles–Atherton models to take into account hysteresis phenomenon for finite element analysis. *Journal of Magnetism and Magnetic Materials*. 2003;261(1-2): 139-160.
[117] Suzuki T, Matsumoto E. Comparison of Jiles–Atherton and Preisach models extended to stress dependence in magnetoelastic behaviors of a ferromagnetic material. *Journal of Materials Processing Technology*. 2005;161(1-2): 141-145.